CELL SURFACE INTERACTION ON A MULTI - SCALE

_

BY

SARAH AKUA MENSAH

A THESIS

SUBMITTED TO THE AFRICAN UNIVERSITY OF SCIENCE AND TECHNOLOGY

ABUJA – NIGERIA

IN PARTIAL FULFILLMENT OF THE REQUIREMENTS FOR THE

AWARD OF MASTER OF SCIENCE IN (MATERIALS SCIENCE AND ENGINEERING)

SUPERVISOR: PROF. WINSTON OLUWOLE SOBOYEJO

DEDICATION

With love,

this thesis is dedicated to my family,

my mother, Miss. Theresah Love Aggrey,

and my dearest son Justin

ACKNOWLEDGEMENTS

My time in African University of Science and Technology has really been a blessing. I express my profound gratitude to the almighty God and everyone who has helped me along the way.

First of all, my most sincere gratitude and appreciation has to be given to my supervisor, Professor Wole Soboyejo, for his fatherly guidance, support, and encouragement; for his being gentle, kind, wise and energetic all the time. Thank you for your confidence in me and giving me opportunities, I could not have dreamt of.

My sincere appreciation goes to mum. You have always been my best friend. You are only next to God in my life. Thank you for your encouragement when I need it most. Thank you dad for all the hopes you had in me and for all the memories I still treasure. I only wish you could have seen me today.

I cannot end without saying a big thank you the African University of Science and Technology for giving me the platform to attain academic excellence and to the Nelson Mandela Institutes for providing me with the scholarship which made my MSc degree a possibility. To the African Development Bank, I say God bless you “Ayekoo” for the financial support in my MSc education.

Finally, I would like to express my heartfelt gratitude to all the PhD candidates and MSc students who have contributed to my academic success in any way. Thank you Danyuo Yiporo and Chukuemeka J. Ani for your immense contribution to my thesis.

ABSTRACT

The increasing rate of cancer patients worldwide, and especially Africa has led to numerous efforts to battle it. One approach to this has been localized drug delivery to reduce the quantity of drugs needed for therapeutic effect. Poly-di-methyl-siloxane (PDMS) is an elastomer with much focus on it as a microfluidic device. PDMS is one polymer of choice for localized drug delivery due to its biocompatibility, transparency, and ease of fabrication. However, its highly hydrophobic nature does not allow it to be used without modification. This work presents results of experimental and computational methods for PDMS surface modification. Also computational results of shear assay model for the effects on surface modification on cell adhesion is present. Modifying the surface of the PDMS was done by varying the mix ratio and curing temperatures after fabrication. The results from the experiment shows that low base to curing agent ratio and increasing curing temperature gives a highly stiff PDMS. Also, the PDMS treatment via boiling water and Ultraviolet Ozone (UVO) methods makes it hydrophilic with the generation of hydroxyl (OH) group on the substrates. These studies provided understanding of cell-surface interaction on a multi-scale. Morphological studies with Scanning Electron Microscope (SEM) reveal a layer and textured featured formed on UVO treated and PLGA coated PDMS. Shear assay model showed that cells on modified PDMS surface low energy release rate on application of shear load. This signifies that cells adhered to the modified surfaces better, thus could not be easily detached.

Table of Contents

LIST OF FIGURES

LIST OF TABLES

1.0 CHAPTER ONE

1.1 INTRODUCTION

The treatment of injury, disease and congenital malformation from traditional to scientific has been part of the human experience. Better ways are sought to improve human life. One disease that is currently taking human lives is cancer. Cancer is second only to cardiovascular disease [1, 2], and with current trends is likely to become the leading cause of death globally by 2030 [1].

In a quest to battle this globally threatening disease, research is being done to improve on conventional methods of detection and treatment [3-6]. This is to reduce the various side effects that accompany existing methods based on surgical procedures, radiation therapy, including bulk systemic chemotherapy. It is important to explore alternative approaches that can reduce the killing of normal or healthy cells during the cancer treatments.

An emerging field, tissue engineering, which provides an approach for the repair and fabrication of tissue from living cells [7] offers a better approach to cancer treatment. Soft tissue engineering plays a vital role in the treatment of cancer through implantable device. Implantable cancer treatment device enables localized drug delivery [6, 8]. This reduces the quantity of drug that is needed to have therapeutic effect significantly. Thus potential side effects of localized cancer drug delivery become much less than bulk systemic chemotherapy.

In localized cancer drug delivery, one polymer which has been used as a packaging material for controlled drug release is poly-di-methyl-siloxane (PDMS) [9]. PDMS is a biocompatible polymer, according to the United States Food and Drug Administration (US FD) and after some toxicity studies [10, 11], it has been approved for applications in implantable biomedical devices in humans [12, 13]. The challenge, however, lies in the physiochemical properties of PDMS surfaces, which may affect proper cell function, leading to poor integration of biomedical implants.

Even though some general correlations between the physiochemical properties of a given surface and its performance as a support for cell adhesion and growth have been established, there is limited understanding of the multi-scale interactions that lead to cell adhesion. There is therefore the need to study the effects of cell adhesions at multiple scales (nano, micro and meso).

1.1.2 Objectives

There are still significant unresolved issues that must be resolved to enable the design of improved adhesion between cells and implantable drug delivery device [15, 16]. These must be resolved to ensure improved integration between PDMS and biological cells/tissue. This will be done by the fabrication of PDMS and the engineering PDMS surfaces to make them more suitable for applications in an implantable cancer treatment device. This will be achieved by the use of surface modification and extra-cellular matrix (ECM) coating techniques. The adhesion between PDMS and the ECM proteins (that are secreted between cancer cells membranes and substrates will also be measured using

shear assay techniques. The implications of the results will also be explored for the design of coated and textured PDMS surfaces in an implantable drug delivery device.

1.1.3 Scope of work

Chapter 1 provides a brief introduction to the scope of the problems and the current work. Following the introduction in Chapter 1, a literature review will be presented in Chapter 2. This survey will provide an overview of microfluidic devices for shear assay measurement, the structure and properties of PDMS, and the effects of coatings and surface texture on adhesion and cell/surface integration. The theory of adhesion will also be explored along with Atomic Force Microscopy (AFM) and shear assay techniques for the measurement of adhesion.

Chapter 3 will present the experimental techniques. These will include: PDMS fabrication methods; ECM coating and surface modification technique. AFM and shear assay techniques will also be presented for the measurement of cell adhesion.

Chapter 4 will use computational modelling to the effects of soft and hard coatings on smooth or grooved PDMS surfaces. The simulations will explore the effects of coating modulus on micro-groove geometries and stress/strain states that are associated with a pre-stretching groove fabrication technique. The mechanical properties of the individual layers will be incorporated into finite element models that will be implemented using the ABAQUS software package. The simulations will also be used to explore the potential effects of surface geometry and adhesion on cell spreading on coated and uncoated PDMS surfaces.

The results obtained from the experiments and models will be presented and discussed in chapter 5.

Salient conclusions arising from this work will be presented in Chapter 6 along with suggestions for the future work.

1.2 Reference for Chapter One

[1] P. Boyle and B. Levin, "The World Cancer Report", World Health Organization, International Agency for Research on Cancer (IARC) Press, Lyon. 112, 2008.

[2] J. Mackay and G. A. Mensah. "The Atlas Of Disease and Stroke", WHO In Collaboration with the Centers for Disease Control and Prevention, ISBN-13 97892415, 2004.

[3] Q. A. Pankhurst, J. Connolly, S. K. Jones and J. Dobson. "Topical Review: Applications of Magnetic Nanoparticles in Biomedicine". Journal of Physics D: Applied Physics, 36-R167–R181, June 2003.

[4] W. Zhou, W. He, and S. Zhong. "Biosynthesis and Magnetic Properties of Mesoporous Fe_3O_4 Composites," Journal of Magnetism and Magnetic Materials, vol. 321, pp 1025–1028, 2009.

[5] A. Petri-Fink, M. Chastellain, L. Juillerat-Jeanneret, A. Ferrari and H. Hofmann. "Development of Functionalized Magnetic Nanoparticles for Interaction with Human Cancer Cells," Biomaterials vol. 26, 2685, 2005.

[6] Y. Oni, C. Theriault, A. V. Hoek and W. O. Soboyejo, “Effects of Temperature on Diffusion from PNIPA-Based Gels in a BioMEMS Device for Localized Chemotherapy and Hyperthermia,” Mater. Sci. and Eng. C., vol. 31, pp. 67-76, 2011.

[7] J. B. B. Sascha Abramson, Harold Alexander, Serena Best, J. C. Bokros, L. L. H. Andr´E Colas, Stuart L. Cooper, Jim Curtis, Axel Haubold, J. A. J. Robert W. Hergenrother, Allan S. Hoffman, Jeffrey A. Hubbell, C. M. Martin W. King, Joachim Kohn, Nina M. K. Lamba, Robert Langer, S. A. V. Robert B. More, Nicholas A. Peppas, Buddy D. Ratner, and and I. V. Y. Andreas von Recum, Steven Weinberg, “Classes of Materials Used in Medicine,” in Biomaterials Science: An introduction to materials in medicine, 2nd Edition, J. E. L. Buddy D. Ratner, Allan S. Hoffman, Frederick J. Schoen, Ed. Elsevier Academic Press, p. 67.

[8] G. Fu and W. O. Soboyejo, “Swelling and Diffusion Characteristics of Modified Poly (N-Isopropylacrylamide) Hydrogels,” Mater. Sci. and Eng. C., vol. 30, pp. 8-13, 2010.

[9] Y. Danyuo, J. D. Obayemi, S. Dozie-Nwachukwu, C. J. Ani, O. S. Odusanya, Y. Oni, N. Anuku, K. Malatesta and W. O. Soboyejo, “Prodigiosin Release From an Implantable Biomedical Device: Kinetics of Localized Cancer Drug Release,” J. Mater. Sci. Eng. C (MSEC), Elsevier, vol. 42, no. 1, pp. 734–745, 2014.

[10] G-H. Hsiue, S-H. Hsu, C-C. Yang, S-H. Lee, I-K. Yang, “Preparation of controlled release ophthalmic drops, for glaucoma therapy using thermosensitive poly-N-isopropylacrylamide,” Biomaterials, vol. 23, pp. 457-462, 2002.

[11] Y. Matsumaru, A. Hyodo, T. Nose, S. Ito, T. Hirano, S. Ohashi, “Application of thermosensitive polymers as a new embolic material for intravascular neurosurgery,” J Biomater Sci. Polym Ed. 7, pp. 795-804, 1996.

[12] P-J. Wipff, H. Majd, C. Acharya, L. Buscemi, J-J. Meister, B. Hinz, “The covalent attachment of adhesion molecules to silicone membranes for cell stretching applications,” Biomaterials, vol. 30, pp. 1781-1789, 2009.

[13] Dow Corning Healthcare Product Selection Guide, “Advancing Healthcare through Material Innovations,” U.S. FDA-Registered (CFN 1816403). Form No. 51-988E-01(©2001, 2002, 2003, 2007, 2013 Dow Corning Corporation) 2-19.

[15] K. J. Painter, N. J. Armstrong, and J. a Sherratt, “The impact of adhesion on cellular invasion processes in cancer and development,” J. Theor. Biol., vol. 264, no. 3, pp. 1057–67, Jun. 2010.

[16] C. Hassler, T. Boretius,T. Stieglitz, “Polymers for Neural Implants,” Journal Of Polymer Science: Part B: Polymer Physics, vol. 49, pp 18–33, 2011.

2.0 CHAPTER TWO: LITERATURE REVIEW

2.1 Introduction

In-vitro studies are useful to understanding human biology and disease. By culturing cell models, various studies can be made to better understand the human biology and disease. Some models have been made *in-vitro* to incorporate endothelial, bone tissue cells, and others [1]. One important technology is microfluidics for cell culturing, which allows for the mimicking of the complex structure of organs.

In an effort to understand multi-scale cell/surface interactions, this chapter presents a review of prior work and on cell/surface interactions, focusing on PDMS substrates. The chapter also presents a microfluidic system for localized cancer drug delivery. The results of prior work on the surface modification and mechanical/surface properties of PDMS are also presented. Finally, the chapter examines the effects of surface morphology and surface chemistry on cell/surface interaction.

2.2 Microfluidic systems

Microfluidic systems are increasingly being utilized as cell culture platforms. Microfluidic is a science and technology of systems that process or manipulate small (10–9 to 10–18 litres) amounts of fluids, using channels with dimensions of tens to hundreds of micrometers. The first applications of microfluidic technologies have been in analysis, for which they offer a number of useful capabilities: the ability to use very small quantities of samples and reagents, and to carry out separations and detections with high

resolution and sensitivity; low cost; short times for analysis; and small footprints for the analytical devices. [2]

The possibility of delivering reagents to defined domains of cell surface or the interior of cell instead of exposing them to the whole cell[1] makes microfluidics essential in performing targeted drug delivery for cancer treatment. The elastomer often used to fabricate microfluidic devices for cell culture experiment is PDMS, among various microfluidic systems. This is by virtue of its simple fabrication process and its much useful material attributes.

2.3 PDMS

PDMS is a flexible elastomeric polymer that is an excellent material for the fabrication on microfluidic device [3]. It has enormous advantages such as easy fabrication, low cost, practical scalability, optical transparency, and gas permeability. The elasticity of PDMS matrices allows the integration of pressure-driven valves and pumps with microfluidic channels, making execution and automation of complex chemical or biological processes within a single microfluidic chip possible[4]. For biomedical applications, the important features of PDMS are physiological indifferences, excellent resistance to biodegradation, ageing and high biocompatibility [5]. Studies have showed that material properties remained unchanged after 2 years of implantation with no biodegradation [6]. In biomedicine it is often utilized as encapsulation or substrate material [5].

In spite of all the strengths of PDMS, which makes it a robust platform for “cell on chip” technology, it has a disadvantage of being hydrophobic. The hydrophobicity of PDMS limits cell attachment and growth. This limitation often prevents the use of PDMS

substrate materials for cell adhesive culture, if without additional treatments such as cell adhesion factor and expensive surface modification procedures[7].

In view of this the current work is focused on modifying PDMS surfaces to improve cell/surface interaction for their use as implantable device to provide insights for the integration of drug eluting cancer treatment device into the human body.

2.3.1 Surface Modification of PDMS

Significant research has been done to modify the physical and chemical properties of PDMS substrates [3, 8, 9]. Some of the techniques that can be used to modify PDMS surfaces include: UV-ozone radiation [9], oxygen plasma treatment [10], self-assemble monolayer coating [11], or polymer/peptide grafting [12] techniques.

Park et al. (2012) have explored the surface chemistry modification of PDMS elastomers with boiling water treatment. This was found to be an effective, inexpensive and convenient way of enhancing the cytophilicity of PDMS. The mechanism is by generating hydrophilic hydroxyl cell binding sites on the surfaces of hydrosilylation cured PDMS elastomers. What makes this method more convenient is the elimination of equipment required for conventional vapor plasma or UV-ozone methods and the possibility of being performed in virtually any laboratory. The efficacy of this method was demonstrated on cell culture using Human mesenchymal stem cells (hMSCs) by showing that the boiling water treatment introduces surface hydroxyl groups to enhance cell attachment to an extent sufficient to alter morphology and gene expression levels

The reaction at the near end of the PDMS elastomer surface in boiling water has been proposed as below [13]:

$$(\text{-SiH}) + H_2O \xrightarrow{Pt} (\text{-Si-OH}) + H_2\uparrow \quad \text{.....(1)}$$

The SiOH group formed is likely to create polar hydrogen bonding sites that would offer relief from the strong hydrophobic environment of PDMS. This will consequently make the surface 'cell-friendly' and promote cell adhesion [7].

Another approach to modifying PDMS surface, is where wrinkles with a well- ordered checkerboard pattern was created using dip-coating of poly (methyl methacrylate) (PMMA) on a UV-ozone treated PDMS substrate [14]. This pattern was found to be induced by swelling the substrate surface with acetonitrile and the alignment. It was achieved by wrapping the substrate around a pipe. Also, the compressive stress in the PMMA coating on the substrate also induced wrinkles. These two mechanisms originating wrinkles resulted in the formation of a checkerboard pattern. This approach resulted in PDMS surface modification at the micro-scale. The size of a unit cell of such a checkerboard pattern was typically about 86 μm wide, 142 μm long and 10 μm deep [14]. The images of wrinkles with a checkerboard pattern described are presented in Figure 2.1

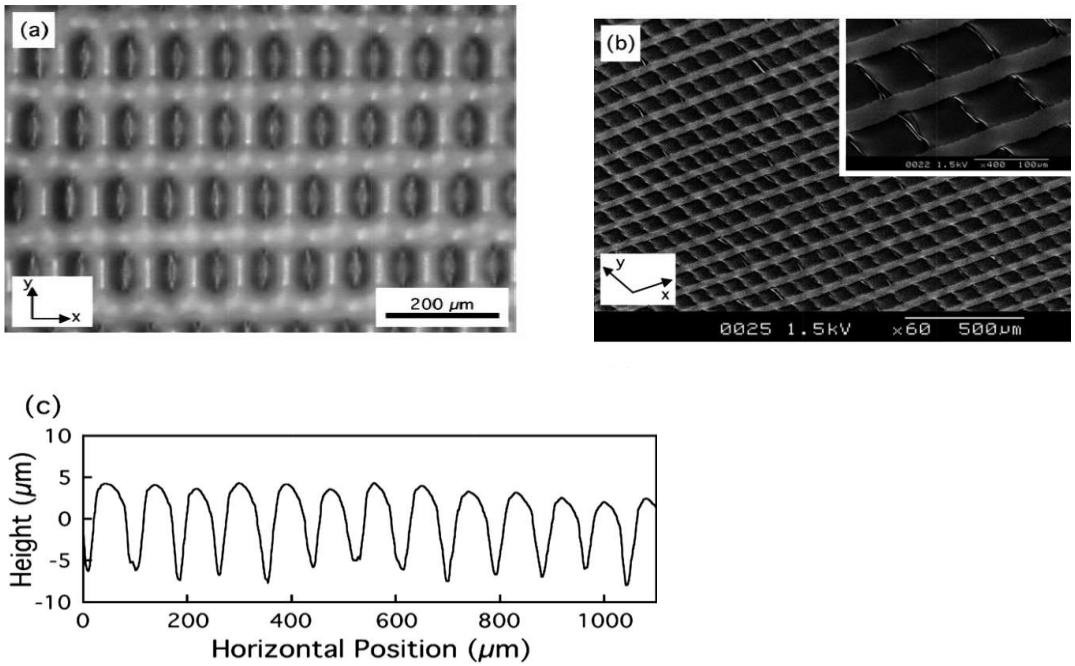

Figure 2.1: (a) light (b) scanning electron microscope images of wrinkles with a checkerboard pattern. (c) A surface profile measured using a two dimensional laser surface profiler. (Adapted from Masashi Watanabe) [14]

2.3.2 Mechanical characterization of PDMS

When polymers are used for the fabrication of biomedical implants, target specifications usually concern the flexibility and stiffness, compared to the surrounding tissue [5]. Elastomers are known to have varying mechanical properties, based on their curing and operational temperatures [15]. The resistance of an elastomer to axial deformation is characterized by Young's modulus [16].

High modulus substrates have been found to be a key factor in determining cell behavior, although it is by no means always so [17]. Some studies have showed that the Young's modulus plays an important role in regulating cellular function, such as proliferation [18], migration [19], differentiation [20], and apoptosis [21]. It is, therefore, important to characterize the mechanical properties of PDMS substrate to in order to study their

effects on cellular function. During cell/surface interactions, the ECM and the substrate provide physical support for cell anchorage. The cells also sense the substrate stiffness and the stiff nesses of nano- and micro-posts, as well as the ECM coatings on the textured surfaces [17].

In as much as curing and operational temperatures results in varying mechanical properties, there is limited range of data regarding the variation in mechanical properties of bulk PDMS with curing temperature by Sylgard 184. However there have been some studies on the mechanical characterization of bulk Sylgard 184 [15]. In these studies, the mechanical characterization of bulk Sylgard 184 has been explored. A linear relationship was found between the curing temperature and Young's modulus [15]. As the curing temperature increases from room-temperature ($25^{o}C$) to $200^{o}C$, the Young's modulus increases from 1.32 to 2.97 MPa. A decreasing linear trend was also found between curing temperature and ultimate compressive (UCS) and tensile strength (UTS). It was from about 5 to 3.5 MPa and 51 to31 MPa respectively for UTS and UCS. This work provides a quantitative data for designs employing Sylgard 184 PDMS as engineering substrate material. The influence of curing temperature on the mechanical properties of Sylgard 184 is summarized in table 2.1

The mechanical properties of the substrate material underpin the process of cell recognition of the material [22]. The ability of cells to react to mechanical properties of the substrate is referred to as mechano-sensing [22]. During mechano-sensing, there is both the action of the material on the cell and the action of the cell on the material [23].

Harris et al. [24] first observed experimental evidence of mechano-sensing over 30 years ago when they measured cell contractile forces on flexible rubber membranes.

Table 1.1: Influence of curing temperature on the mechanical properties of PDMS [15]

Temperature (^{o}C)	Young's modulus, E (MPa)	UTS (MPa)	UCS (MPa)
25	1.32±0.007	5.13±0.55	51.7±9.60
100	2.05±0.12	6.25±0.84	40.1±4.30
125	2.46±0.16	7.65±0.27	36.8±3.84
150	2.59±0.08	5.24±0.82	28.4±4.46
200	2.97±0.04	3.51±1.11	31.4±2.04

2.4 Cell/surface interaction

The interactions between the cell and the substrate determine the cell adhesion, motility, growth and fate [25]. The cell/surface interaction is significantly influenced by the surface topography and cell behavior [26, 27]. Following adhesion and cell contact with the surface, cell spreading, proliferation and mineralization result in the formation of tissue integrated implant structures [28].

2.4.1 Cell

The cell is the basic unit of biology [29]. It is composed of nucleic acids, proteins, and other large and small molecules and is held together by cell-to-cell junctions to form tissue [30]. Cells are generally known to live in the body and in the cell culture laboratory. They exist, either in transient or long term contact with each other, or in adhesion with surfaces [31]. These surfaces are either implanted biomaterials or natural.

For cells to adhere to surfaces, they are often patterned with chemical or topographic features [31]. There is a controversy about the likelihood of a cell reacting to topography other than chemical differences [31]. However, the overall consensus in recent years suggests that cells react significantly to the mechanical properties of the substrate, as well as the topography and chemistry of the substrate/coating/ECM complex [32]. These effects will be explored in the study.

The cell is known to be part of a complex and dynamic architecture formed by itself, insoluble macromolecules of the extracellular matrix (ECM), soluble morphogens and growth factors, and surrounding cells [33]. Cells, intercellular (interstitial) substances, especially ECM, and various body fluids make up the basic biological tissue [34].

The ECM is made up of the biological material produced by, residing in between, and supporting cells. Cells are held together by the ECM, which provides physical support and a matrix to which cells can adhere, signal to each other, and interact. The components of ECM are fibers (collagen and elastin) and a largely amorphous inter-fibrillary matrix (mainly proteoglycans, noncollagenous cell-binding adhesive glycoproteins, solutes, and water). The principal functions of the ECM are [34]:

- Mechanical support for cell anchorage
- Determination of cell orientation
- Control of cell growth
- Maintenance of cell differentiation

- Scaffolding for orderly tissue renewal
- Establishment of tissue micro-environment
- Sequestration, storage, and presentation of soluble regulatory molecules

Cells primarily interact with surfaces through the creation of attachment points linking the cytoskeleton (the cell's mechanical framework) to extracellular binding sites [35]. ECM transmits environment signals to cell; therefore cell-ECM bio-interface is an indispensable part for cell's life [17]. In Figure 2.2 the stages of cell surface adhesion are presented.

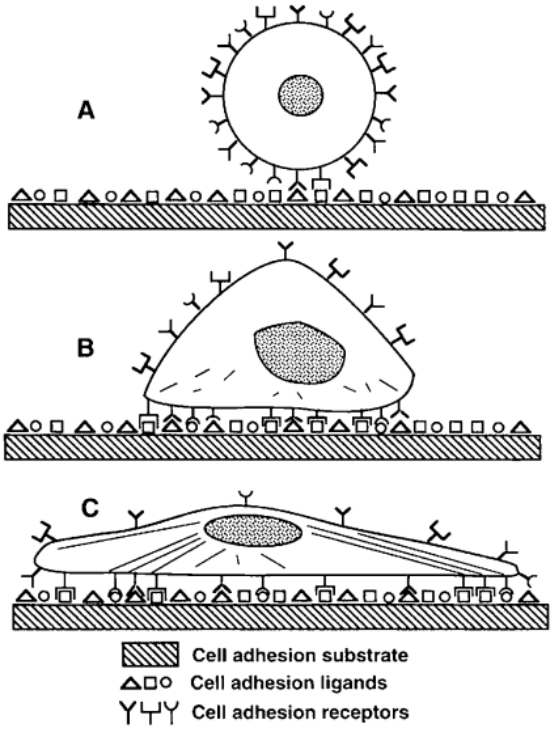

Figure 2.2: (A) initial contact of cell with solid substrate (B) Formation of Receptor-Ligand Bonds; (B) Signal Transmission from Focal Adhesion Sites to Cell's Nucleus: (C) Cell Deformation and Cell Spreading by cytoskeletal reorganization for increased attachment (adapted from Frederick J. Schoen and Richard N. Mitchell) [34]

In figure 2.2 (A) the interactions of cell with foreign surface are mediated by integrin receptors with adsorbed adhesion proteins that sometimes change their biological activity when they adsorb [34]. The cell has been shown as a circular space with a bilayer membrane in which the adhesion receptor protein molecules (the slingshot-shaped objects) are partly embedded. The proteins in the extracellular fluid are represented by circles, squares, and triangles. The receptor proteins recognize and cause the cell to adhere only to the surface-bound form of protein; the one represented by a solid circle will adhere to proteins in the extracellular fluid are represented by circles.

Generally, the cytoskeleton and the focal adhesions are responsible for internal organization, shape and cell mobility [36]. Actin microfilaments and micro-tubules, which make up the cytoskeleton, provide support and serve to maintain cell shape. Cell/substrate contact occurs as a result of focal adhesion. They tend to ensure cell/substrate contact [37].The focal adhesion involves integrins bound to actin filaments in the cytoskeleton through various adhesion proteins that include vinculin (Figure 2.3)

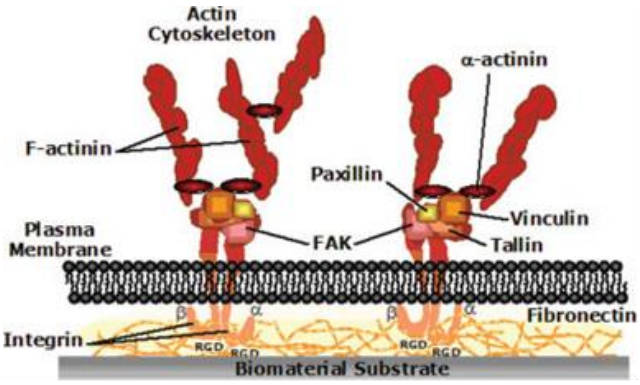

Figure 2.3: Schematic representation of cell adhesion to a biomaterial substrate (focal adhesions and several associated cell proteins are also shown in the schematic) (Adapted from J. Chen, S. Mwenifumbo, C. Langhammer, J. Mcgovern, M. Li, A. Beye, and W. O. Soboyejo) [36]

2.4.2 Cell surface interaction on a multi-scale

Modifying surface properties over multiple length scales is critical in the optimization of a material's performance for a given application [38]. For instance, the adhesive and wetting forces acting at a material interface, can be strongly influenced by the size and shape of the micro- and nano-scale features present [39]. Several relevant length scales exist over which modified surface topography and chemistry of a processed implant can influence cell adhesion and hence integration into the body [32, 40].

The primary behavior of cell on biomedical surfaces, such as cell spreading and adhesion, are influenced by multi-scale surface features. These range from chemisorption and surface energies at the atomic scale [41, 43], to surface roughness and texture at the micro- to meso-scales [44-45]. At the atomic scale, the modification of surfaces through chemical processing increases adhesion. This has been shown to improve the binding of proteins and cells [46]. Protein interactions associated with cell signaling which regulates cell adhesion, proliferation, and differentiation can also be associated with interactions with nanoscale features. These features can also influence the interactions of individual cell microfilaments and microtubules in the form focal adhesion complexes. This kind of interaction is showed in green in Figure 2.4a. At the micron-scale, texturing with features such as grooves, craters, ridges and mountains can increase surface area and enhance focal attachment [36]. This can also lead to the mechanical stretching of cells or contraction to align and organize with the features in a phenomenon known as "contact guidance" [32] (Figure 2.3b). Cells grown on substrates with contact guidance (linear grooves) show organized regrowth and has tendency of decreasing scar tissue formation

during healing [43]. Also, at the macro scale, textured features such as vents, dimples and threads on the implant surface can physically be interlocked.

The overall interaction between cells and surfaces is determined by the multi-scale modification.

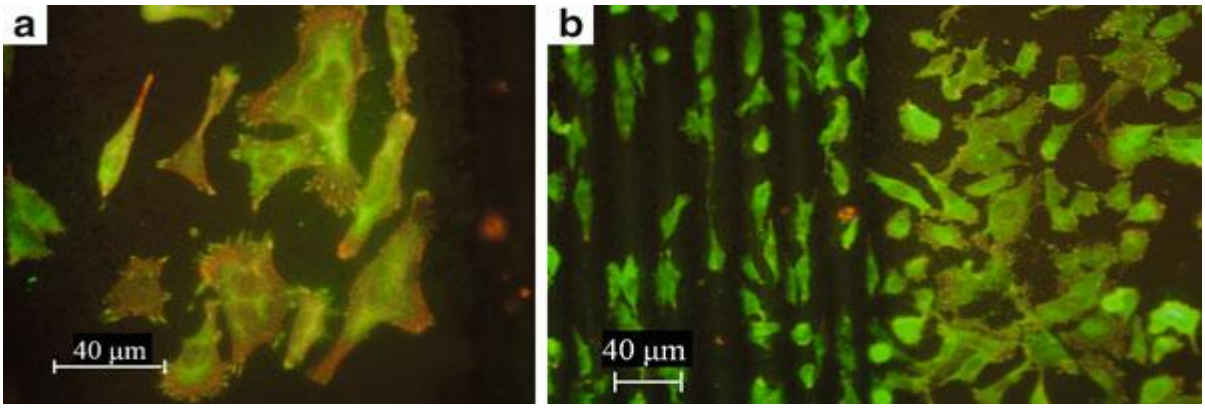

Figure 2.4: (a) Osteoblast-like human osteosarcoma cells. Their vinculin and focal adhesion points are stained green and their actin stained red. (b) Contact guidance by linear grooves causes elongation of the cells (left) as compared to the adherence to a polished surface (right). (Adapted from Matthew S. Brown and Craig B. Arnold) [38]

2.5 The Effects of Surface Morphology on Cell/Surface Interaction

Surface properties of biomaterials which include physiochemical properties of surface hydrophobicity, morphology, roughness, surface modification and coatings can affect cell adhesion, attachment, proliferation and differentiation of cell [47].

2.5.1 Roughness

As part of the impact, that surface modification has on implants on a multi – scale, surface roughness and texture, at the micro- to meso-scale [48] is significant to final adhesion. This significance comes to play in the initial interactions between cells and

biomaterials occurring on a multi-scale, and subsequently playing an important role in final cell adhesion [42]. Studying the role of surface roughness in cell/surface interactions is critical because experimental studies have shown that surface characteristics of the implant material play an important role in tissue response [49-51]. Surface roughness also modulates the biological response of tissues in contact with implant.

In recent times, micro-grooves have been used to modify the surface characteristics of biomaterials and influence the behavior of cells [43, 52]. Micro-grooves have also been found to increase contact guidance [41-43, 53-55]. By physically roughening surfaces, it has been shown that the soft tissue response is sensitive to variation in topology and surface morphology [56, 57]

2.5.2 Surface Texture

The surface texture of an implant is a critical variable in the determination of soft tissue response to a material. S.R. Taylor [58] demonstrated that implanting textured surfaces altered the interfacial cells and kinetics of fibrous capsule development. These interfacial cells associated with textured interfaces displayed increase in adhesion.

2.6 The Effects of Surface Chemistry on Cell/Surface Interaction

Implants are covered in a protein – enriched film upon contact with blood which enables adhesion to the surface via weak temporary bonds or stronger permanent covalent bonds [59]. Collagen, fibronectin and vitronectins are proteins that are likely to adsorb onto the surface of optimal hydrophobicity to enhance adhesion [46]. Prior work [47, 48] has shown that the patterning of biomaterials surfaces with proteins and peptides can increase

the level of cell adhesion. Also, cells respond differently to variations in surface chemistry [60]. They can also distinguish between proteins or even peptides of few amino acids [60].

Alterations in surface chemistry will effectively influence protein adsorption and conformation, and ultimately initial cell attachment. This alteration is essential because the surface of an implant determines which proteins adsorb to it and the orientation of attachment [61].

The most concentrated protein in blood is Albumin (66kDa). It generally dominates the initial cell/surface interactions. However, fibronectin (340kDa) which is lower in concentration and arrives late at an implant surface due to its size, usually dominates the surface protein coating because of its higher affinity for surface [62, 63]. Adsorbed adhesive proteins mediate the attachment and activation of neutrophils, macrophages, and other inflammatory cells.

Another key factor that governs cell response on a substrate is hydrophobicity [64]. The surface hydrophobicity is determined by the measurement of contact angle through water spread of a droplet on a surface. High contact angle signifies hydrophobic surfaces. Optimal hydrophobicity is likely to allow the adsorption of proteins of cell adhesion, such as collagen, fibronectin, and vitronectins [47]. However, high hydrophobicity and hydrophilicity suppresses the cell adhesion because of the less protein adsorption onto it [65, 66]

2.7 Methods for Studying Cell/Surface Adhesion

The adhesion between cells and biomaterials is very important for the integration of biomedical implants [67]. The significance of the cell/surface adhesion has stimulated significant research efforts [68-73] in the development of experimental techniques for the measurement of cell adhesion. Since cell adhesion has a significant effect on cellular functions, such as proliferation, differentiation, etc., quantitative measurements of cell adhesion provide us with insights into these cell functions. It is also important to note that these cell functions occur when cells attach to a substrate and begin to spread and form an organized actin cytoskeleton and complex transmembrane signaling regions [74]. In any case, cell adhesion is measured using techniques such as micro-pipette aspiration [75]; laser tweezer measurements [76]; atomic force microscopy (AFM) measurement [77,78]; cell traction measurement [78], and shear assay techniques[79] (Figure 2.5 -2.8).

2.7.1 Micro-pipette Aspiration

Measurement of large number of cells gives statistically reliable information of cell adhesion. However, direct measurement of the adhesion force of single cells is still challenging and today's techniques typically have an extremely low throughput (5–10 cells per day) [80]. Rita et al [80] introduced a computer controlled micropipette mounted onto a normal inverted microscope for probing single cell interactions with specific macromolecules. The Micropipette adhesion assay was developed in 1998 to measure two-dimensional (2D) receptor-ligand binding kinetics [81].The assay uses a human red blood cell (RBC) as the adhesion sensor. It also uses micro-manipulation to bring the RBC into contact with another cell that expresses the other interacting molecule with precisely controlled area and time to enable bond formation.

The processes involved in the micropipette technique are described by Hochmuth [75] is as follows: a nearly inflated red cell or lipid bilayer vesicle is aspirated into a small micropipette until the surface of the membrane outside of the pipette is spherical; a bead is then attached to the membrane at a point that is diametrically opposite to the mouth of the pipette; the deflection of the bead is proportional to the force exerted on it and the spring constant for this deflection (force per unit deflection) can be adjusted by adjusting the suction pressure (the device can measure pN-level force). It is ideally suited for measuring molecular bond forces

A schematic of the micropipette aspiration system is presented in Figure2.7. This shows a common application where a cell suspended in a saline solution is partially aspirated into the mouth of the pipette. The round shape occurs either naturally in the case of white cells or spontaneously when cells are detached from a surface.

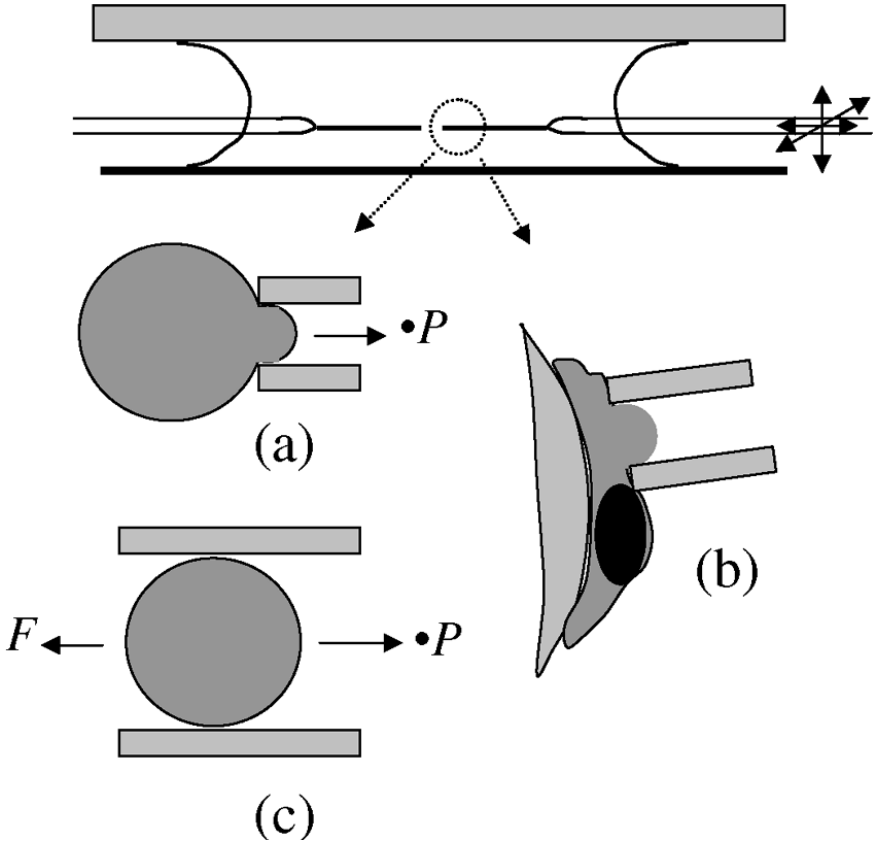

Figure 2.5: Two micropipettes in a chamber. A pneumatic micromanipulator controls the movement of a micropipette along three orthogonal axes. (a) A spherical cell being aspirated into a micropipette with a suction pressure ΔP. (b) An attached cell being aspirated into a pipette. (c) A closely "fitting cell or bead moving freely in a pipette like a piston in a cylinder. When static, the suction pressure times the cross-sectional area of the pipette equals the attachment force F [75].

2.7.2 Laser tweezers

The laser tweezers usually are limited to the measurement of small forces on the order of 50 pN, although more powerful lasers and better alignment of the system can produce forces that are an order of magnitude larger than this [75].

2.7.3 AFM

Force microscopy during atomic force microscopy (AFM) is a powerful tool for probing the mechanical behavior of living cells: by allowing 3-D manipulation of cells with nanometric resolution with simultaneous measurement of the applied force with pN sensitivity [82]. The use of AFM for cell adhesion measurement employs a sharp tip, attached to a cantilever for probing cell. Upon probing, deformation occurs on the cell and the tip is then used to estimate the force applied and the stiffness of the cell. Radmacher et al. [84, 85] used AFM to investigate the viscoelastic properties of human platelets. The set-up is shown in Figure 2.8.

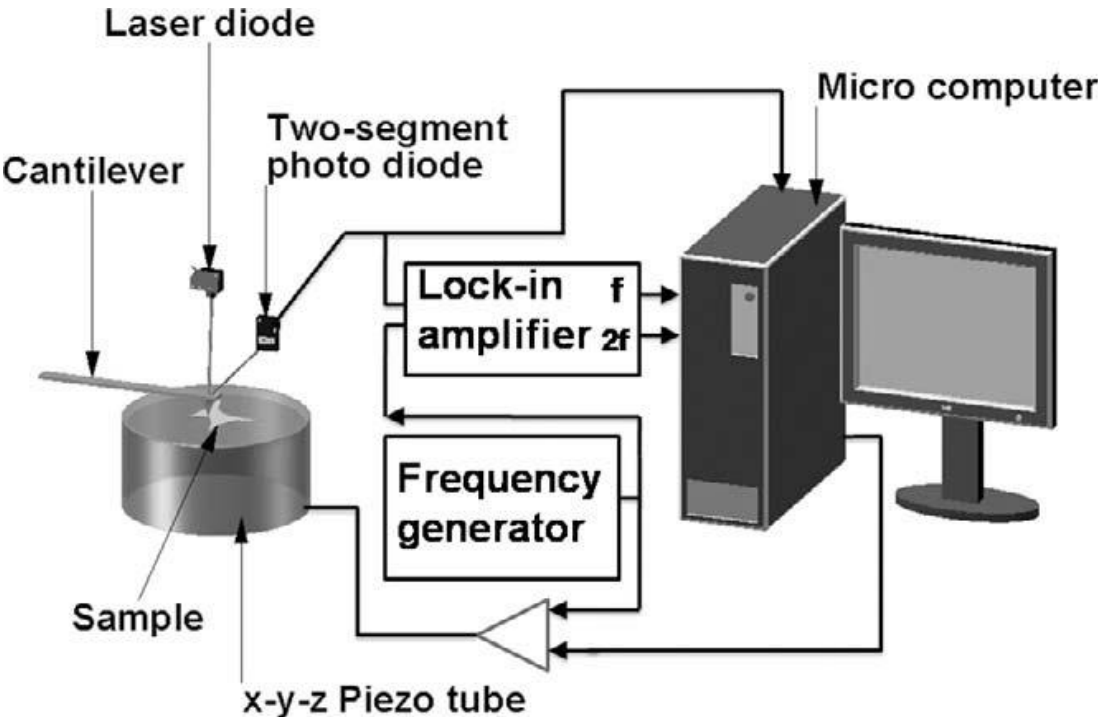

Figure 2.6: A schematic of an AFM setup, which incorporates optical lever detection and includes electronics for investigating viscoelastic properties of samples. (Adapted from Radmacher et al. [84]

2.7.4 Cell Traction Measurements

In order to survive and grow, cells in culture must adhere to a solid substrate. This makes cells in culture typically anchorage dependent [86]. Cells develop tension via actomyosin interactions inside cells, which is then transmitted to the underlying substrate through focal adhesion located on substrate [87]. Measurement and characterization of this traction force leads to the understanding of cellular and molecular mechanism of fundamental biological processes, since cells use it to organize ECM, maintain shape, to probe physical environment, and generate mechanical signals [88].

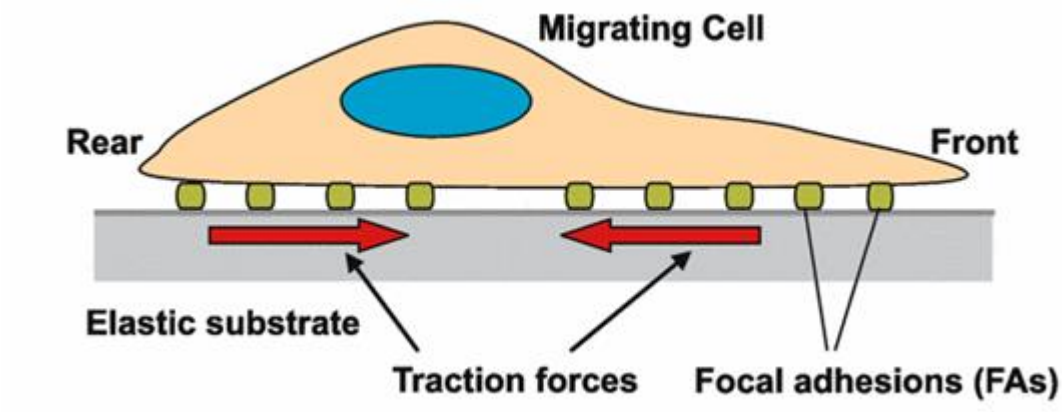

Figure 2.7: A representation of cell traction forces. The forces are the cell tension that is generated by actomyosin interactions and transmitted to underlying substrate through focal adhesion

2.7.5 Shear Assay Measurement in Parallel-Plate Flow Chambers

The interfacial strengths between the cells and the biomaterials surfaces have been determined using shear assay technique [79]. Shear assay method offers “soft” detachment of cells from biomedical substrates. In this method a parallel flow chamber is used [89–90] and this allows the in-situ observation of cell deformation and detachment

during cell culture where fluid flow across cells in a microfluidic channel [79]. In this method the onset of cell detachment can be determined by monitoring with *in-situ* microscopy.

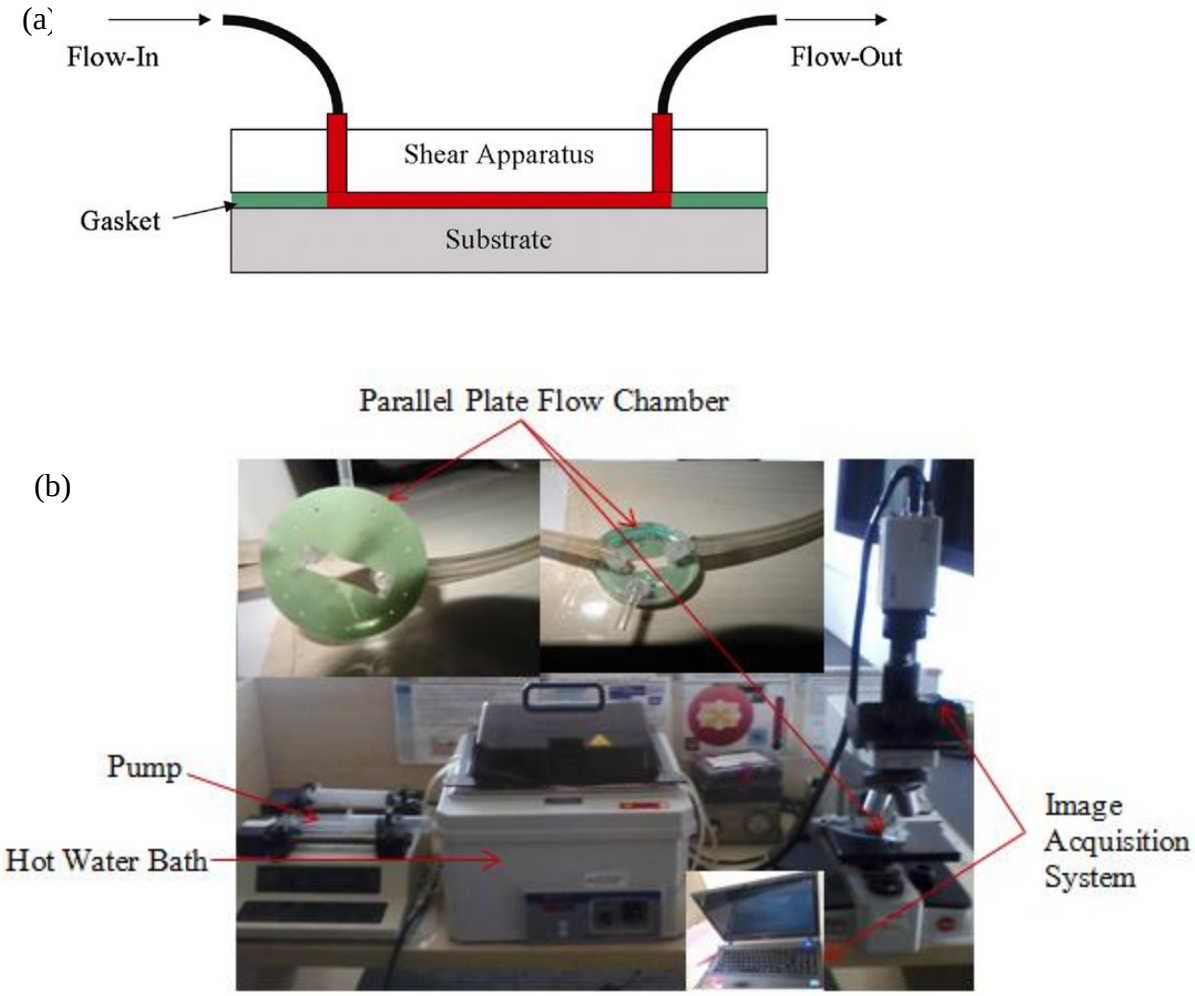

Figure 2.8: The shear assay system: (a) cross-section of shear assay setup, and (b) shear assay experimental setup and flow chamber.

2.8 Summary

A brief introduction to microfluidic systems has been presented in this chapter. Following a review of PDMS, some modification methods used to modify the physical and chemical properties of PDMS, to ensure improved integration between PDMS and biological cells /tissues were introduced. Cell was described before introducing the concepts of multi-scale cell/surface interaction. Cell/Surface interaction was introduced as the interaction between the cell and the substrate that determines the cell adhesion, motility, growth and fate.

2.9 Reference for chapter two

[1] P. S. Dittrich and A. Manz, “Lab-on-a-chip : microfluidics in drug discovery,” Nat. Rev., vol. 5, pp. 210–218, March 2006.

[2] Manz, A. et al., “Planar chips technology for miniaturization and integration of separation techniques into monitoring systems — capillary electrophoresis on a chip,” J. Chromatog. Vol. 593, pp. 253–258, 1992.

[3] P.R.C. Gascoyne, J. Vykoukal, “Particle separation by dielectrophoresis,” Electrophoresis, vol. 23, no. 2 pp. 1973-83, 2002.

[4] G. Sui, J. Wang, C.-C. Lee, W. Lu, S. P. Lee, J. V Leyton, A. M. Wu, and H.-R. Tseng, “Solution-phase surface modification in intact poly (dimethylsiloxane) microfluidic channels,” Anal. Chem., vol. 78, no. 15, pp. 5543–51, Aug. 2006.

[5] C. Hassler, T. Boretius, and T. Stieglitz, “Polymers for neural implants,” J. Polym. Sci. Part B Polym. Phys., vol. 49, no. 1, pp. 18–33, Jan. 2011.

[6] Yoda, R. J. Biomat. Sci: Polym. E 1998, 9, 561–626.

[7] J. Yull, D. Ahn, Y. Young, C. Mo, S. Takayama, S. Hyuck, and S. Lee, “Surface chemistry modification of PDMS elastomers with boiling water improves cellular adhesion,” Elseveier Sensors Actuators B Chem., vol. 173, pp. 765–771, 2012.

[8] W. Zhang, D. S. Choi, Y. H. Nguyen, J. Chang, and L. Qin, “Studying Cancer Stem Cell Dynamics on PDMS Surfaces for Microfluidics Device,” pp. 1–8, 2013.

[9] K. Efimenko, W. E. Wallace, and J. Genzer, “Surface Modification of Sylgard-184 Poly (dimethyl siloxane) Networks by Ultraviolet and Ultraviolet / Ozone Treatment,” vol. 315, pp. 306–315, 2002.

[10] Bodas, Dhananjay, and Chantal Khan-Malek, “Hydrophilization and hydrophobic recovery of PDMS by oxygen plasma and chemical treatment—An SEM investigation,” Sensors and Actuators B: Chemical, vol.123, no.1, pp. 368-373, 2007.

[11] Makamba, Honest, et al. “Surface modification of poly (dimethylsiloxane) microchannels,” Electrophoresis, vol. 24, no.21, pp. 3607-3619, 2003.

[12] Li, Bin, Jianxin Chen, and James H-C. Wang, “RGD peptide-conjugated poly (dimethylsiloxane) promotes adhesion, proliferation, and collagen secretion of human fibroblasts,” Journal of Biomedical Materials Research Part A, vol. 79, no.4, pp. 989-998 2006.

[13] M.A. Brook, Silicon in Organic, “Organometallic, and Polymer Chemistry,” J. Wiley, New York, 2000, p. xxiv, 680.

[14] M. Watanabe, “Wrinkles with a well-ordered checkerboard pattern, created using dip-coating of poly (methyl methacrylate) on a UV–ozone-treated poly (dimethylsiloxane) substrate,” Soft Matter, vol. 8, no. 5, p. 1563, 2012.

[15] I. D. Johnston, D. K. McCluskey, C. K. L. Tan and M. C. Tracey “Mechanical characterization of bulk Sylgard 184 for microfluidics and microengineering,” J. Micromech. Microeng. vol. 24, (7pp) 035017, 2014.

[16] W. D. J. Callister and D. G. Rethwisch, “Materials Science”, Seventh. New York: John Wiley & Sons, Inc, pp. 1–975, 2007.

[17] J. Li, D. Han, and Y. Zhao, “Kinetic behaviour of the cells touching substrate : the interfacial stiffness guides cell spreading,” pp. 1–11, 2014.

[18] E. Hadjipanayi, V. Mudera, R. Brown, “Close dependence of fibroblast proliferation on collagen scaffold matrix stiffness,” J. Tissue Eng. Regen. M. vol. 3, pp. 77–84, 2009.

[19] C. M. Lo, H. B. Wang, M. Dembo, and Y. Wang, “Cell movement is guided by the rigidity of the substrate,” Biophy. J. vol. 79, pp. 144–152, 2000.

[20] A. J. Engler, S. Sen, H. L.Sweeney, and D. E.Discher, “Matrix elasticity directs stem cell lineage specification,” Cell, vol. 126, pp. 677–689, 2006.

[21] R. W. Tilghman et al., “Matrix rigidity regulates cancer cell growth and cellular Phenotype,” PLoS One 5, e12905, 2010.

[22] M. Ventre, F. Causa, and P. a Netti, “Determinants of cell-material crosstalk at the interface: towards engineering of cell instructive materials.,” J. R. Soc. Interface, vol. 9, no. 74, pp. 2017–32, Sep. 2012.

[23] V. Vogel, M. Sheetz, “Local force and geometry sensing regulate cell functions,” Nat. Rev. Mol. Cell Biol., vol. 7, pp. 265–275, 2006.

[24] A. K. Harris, P. Wild, D. Stopak, “Silicone rubber substrata: a new wrinkle in the study of cell locomotion,” Science 208, pp. 177–179, 1980.

[25] A. Lazar, F. Borgatti, P. D. Angelo, I. Tonazzini, E. Bystrenova, B. Chelli, P. Greco, P. Stoliar, A. Calo, C. Martini, and F. Biscarini, "Multiscale Morphology of Organic Semiconductor Thin Films Controls the Adhesion and Viability of Human Neural Cells," vol. 98, pp. 2804–2812, 2010.

[26] J. Ma, F. Z. Cui, Q. Y. Xu, "Atomic force and confocal microscopy for the study of cortical cells cultured on silicon wafers," J. Mater. Sci. Mater. Med. 18, pp. 851–856, 2007.

[27] R. G. Flemming, C. J. Murphy, P. F. Nealey, "Effects of synthetic micro- and nano-structured surfaces on cell behavior. Biomaterials," Vol 20, pp. 573–588, 1999.

[28] B. J. Dubin-Thaler, G. Giannone, H. G. Do¨bereiner, M. P. Sheetz, "Nanometer analysis of cell spreading on matrix-coated surfaces reveals two distinct cell states and STEPs," Biophy. J. vol. 86, pp. 1794–1806, 2004.

[29] W. M. Becker, L. J. Kleinsmith, J. Hardin, "The World of the Cell," 4th Edition, San Francisco, CA, 2000.

[30] R. N. M. and F. J. Schoen, "Biology, Biochemistry, And Medicine," in Biomaterials Science: An introduction to materials in medicine, 2nd Edition, J. E. L. Buddy D. Ratner, Allan S. Hoffman, Frederick J. Schoen, Ed., Elsevier Academic Press, p. 246, 2004.

[31] A. S. G. Curtis, "Cell Reactions with Biomaterials: The Microscopies," Eur. Cell. Mater., vol. 1, pp. 59–65, 2001.

[32] A. Curtis, C. Wilkinson, Biomaterials, vol. 18, no.24, p. 1573, 1997

[33] A. M. Kloxin, M. W. Tibbitt, A. M. Kasko, J. A. Fairbairn, K. S. Anseth, "Tunable hydrogels for external manipulation of cellular microenvironments through controlled photodegradation," Advanced Materials, Vol. 22, no. 1, pp 61-66, 2010.

[34] F. J. Schoen and R. N. Mitchell, "Tissues, The Extracellular Matrix, And Cell–Biomaterial Interactions," in Biomaterials Science: An introduction to materials in medicine, 2nd Edition, J. E. L. Buddy D. Ratner, Allan S. Hoffman, Frederick J. Schoen, Ed. Elsevier Academic Press, p. 260, 2004.

[35] M. D. Mager, V. LaPointe, M. M. Stevens, "Exploring and exploiting chemistry at the cell surface," Nature Chemistry, vol. 3, pp. 582–589, 2011.

[36] J. Chen, S. Mwenifumbo, C. Langhammer, J. Mcgovern, M. Li, A. Beye, and W. O. Soboyejo, "Cell / Surface Interactions and Adhesion on Ti-6Al-4V : Effects of Surface Texture," no. 1, pp. 360–373, 2007.

[37] K. Burridge, K. Fath, T. Kelly, G. Nuckolls, C. Turner, "Focal adhesions: Transmembrane junctions between the extracellular matrix and the cytoskeleton," Ann Rev Cell Biol., vol. 4, pp. 487–525, 1988.

[38] M. S. Brown and C. B. Arnold, "Fundamentals of Laser-Material Interaction and Application to Multiscale Surface Modification," in Laser Precision Microfabrication, vol. 135, K. Sugioka, M. Meunier, and A. Piqué, Eds. Berlin, Heidelberg: Springer Berlin Heidelberg, 2010, pp. 91–120.

[39] I. Etsion, J. Tribol. Trans. ASME, vol. 127, no.1, p. 248, 2005.

[40] J. Tan, W.M. Saltzman, Biomaterials , vol. 25, no.17, p. 3593, 2004.

[41] Soboyejo, W. O., et al. “Multi-scale microstructural characterization of micro-textured Ti-6Al-4V surfaces,” Key Engineering Materials, vol.198, pp. 203-230, 2001.

[42] J. Chen, S. Mwenifumbo, C. Langhammer, J. P. McGovern, W. O. Soboyejo, “Cell/surface interactions and adhesion on Ti-6Al-4V: Effects of surface texture. Journal of Biomedical Materials Research Part B: Applied Biomaterials,” vol. 82, no. 2, pp. 360-373, 2007.

[43] W. O. Soboyejo, B. Nemetski, S. Allameh, N. Marcantonio, J. Ricci, “Interactions between MC3T3-E1 cells and textured Ti6Al4V surfaces,” Journal of biomedical materials research, vol. 62, no. 1, pp. 56-72, 2002.

[44] Lim, J. Yul, and J. Henry Donahue, “Cell sensing and response to micro-and nanostructured surfaces produced by chemical and topographic patterning,” Tissue engineering, vol. 13, no. 8, pp, 1879-1891, 2007.

[45] P. Roach, D. Eglin, K. Rohde, and C. C. Perry, “Modern biomaterials: a review—bulk properties and implications of surface modifications,” Journal of Materials Science: Materials in Medicine, vol.18, no. 7, pp. 1263-1277, 2007.

[46] T.G. Vankooten, J.M. Schakenraad, H.C. Vandermei, H.J. Busscher, Biomaterials, vol. 13, no. 13, p. 897, 1992.

[47] Y. Tabata, “Biomaterials Design of Culture Substrates for Cell,” Inflammation and Regeneration, vol. 31, no. 2, pp. 137–145, 2011.

[48] G. C. Menezes, C. N. Elias, M. Attias, F. C. Silvia-Filho, “Osteoblast adhesion onto titanium dental implants,” Acta Microsc, vol. 12, pp.13–19, 2003.

[49] D. M. Brunette, “Effects of surface topography of implant materials on cell behaviour in vitro and in vivo,” In: Hoch HC, editor. Nanofabrication and Biosystems. Cambridge:Cambridge Press; 1996.

[50] K. D. Chesmal, J. Black, “Cellular responses to chemical and morphologic aspects of biomaterial surfaces. I. A novel in vitro system,” J Biomed Mater Res, vol. 29, pp.1089–1099, 1995.

[51] K. D. Chesmal, C. C. Clark, C. T. Brighton, J. Black, “Cellular responses to chemical and morphologic aspects of biomaterial surfaces. I. The biosynthetic and migratory response of bone cell populations,” J Biomed Mater Res, vol. 29, pp. 1101–1110, 1995.

[52] J. L. Ricci, H. Alexander, “Laser microtexturing of implant surfaces for enhanced tissue integration,” Key Eng Mater, 198/199, pp. 179–202, 2001.

[53] J.L. Ricci, J. Charvet, S. R. Frenkel, R. Chang, P. Nadkarni, J. Turner, H. Alexander, “Bone response to laser microtextured surfaces,” In: Davies JE, editor. Bone Engineering. Toronto: Em2, pp 1–11, 2000.

[54] K. Anselme, B. Noel, P. Hardoun, “Human osteoblast adhesion to titanium alloy stainless steel, glass and plastic substrates with the same surface topography,” J Mater Sci: Mater Med, vol. 10, pp. 815–819, 1999.

[55] J. H. Wang, E. S. Grood, J. Florer, R. Wenstrup, “Alignment and proliferation of MC3T3-E1 osteoblasts in microgrooved silicone substrate subjected to cyclic stretching,” J Biomech, vol. 33, pp. 729–735, 2000.

[56] C. A. Homsy and M. S. Anderson, “Functional Stabilization of Prostheses with a Porous Low Modulus Materials System,“ in Biocompatibility of Implanted Materials, D. Williams, Ed., Sector, London, pp. 85-92, 1976.

[57] J. B. Walter and L. G. Chiaramonte, “The Tissue Responses of the Rat to Implanted Ivalon, Etheron, and Polyfoam Plastic Sponges,” Br. 1. Surg., vol. 52, pp. 49-54, 1965.

[58] S.R. Taylor, D.F. Gibbons, “Effect of surface texture on the soft tissue response to plymer implants

[59] B. Kasemo, J. Lausmaa, “Material–tissue interfaces: the role of surface properties and processes,” Environ Health Perspect, vol. 102, no. 5, pp. 41–45, 1994.

[60] U. Hersel, C. Dahmen, H. Kessler, “RGD modified polymers: biomaterials for stimulated cell adhesion and beyond,” Biomaterials, vol. 24, pp. 4385–4415, 2003.

[61] J. S. Hayes, E. M. Czekanska and R. G. Richards, “The Cell–Surface Interaction,”, Adv Biochem Engin/Biotechnology, 2011.

[62] B. Kasemo, J. Gold, “Implant surfaces and interface processes,” Adv Dent Res., vol. 13, pp. 8–20, 1998.

[63] R. G. Richards, “The relevance of implant surfaces in hand fracture fixation,” In: Osteosynthesis in the hand: current concepts, FESSH instructional course 2008, Karger, Basel, pp 20–30, 2008.

[64] H. I. Chang and Y. Wang, “Cell Responses to Surface and Architecture of Tissue Engineering Scaffolds,” pp. 570

[65] Y. Tamada, Y. Ikada, “Fibroblast growth on polymer surfaces and biosynthesis of collagen,” J Biomed MaterRes., vol. 28, pp. 783-789, 1994.

[66] H. Du, P. Chandaroy, S. W. Hui, “Grafted poly-(ethylene glycol) on lipid surfaces inhibits protein adsorption and cell adhesion,” Biochim Biophys Acta, vol. 1326, pp. 236-248, 1997.

[67] B.D. Ratner, Biomaterials Science: An Introduction to Materials in Medicine, Elsevier Academic Press, Amsterdam; Boston, xii, pp. 851, 2004.

[68] L. Chu, L.A. Tempelman, C. Miller, D.A. Hammer, Aiche Journal, vol. 40, pp. 692–703, 1994.

[69] M. A. Griffin, A.J. Engler, T.A. Barber, K.E. Healy, H.L. Sweeney, D.E. Discher, Biophysical Journal, vol. 86, pp. 1209–1222, 2004.

[70] W. Huan, B. Anvari, J.H. Torres, R.G. LeBaron, K.A. Athanasiou, Journal of Orthopaedic Research, vol. 21, pp. 88–95, 2003.

[71] F.Y. Li, S.D. Redick, H.P. Erickson, V.T. Moy, Biophysical Journal, vol. 84, pp. 1252–1262, 2003.

[72] H. Miyata, R. Yasuda, K. Kinosita, Biochimica Et Biophysica Acta-General Subjects, vol. 1290, pp. 83–88, 1996.

[73] H.J. Ra, C. Picart, H.S. Feng, H.L. Sweeney, D.E. Discher, Journal of Cell Science, vol. 112, pp. 1425–1436, 1999.

[74] C.-C. Lee, C.-C. Wu, F.-C. Su, “The Technique for Measurement of Cell Adhesion Force,” Department of Neurology, University Hospital, National Cheng Kung University, Tainan, 701, Taiwan R.O.C., March 2004.

[75] R. M. Hochmuth, “Micropipette aspiration of living cells,” Journal of Biomechanics, vol. 33, pp. 15-22, 2000.

[76] W. Huang, B. Anvari, J. Torres, H. LeBaron, & K. A. Athanasiou, “Temporal effects of cell adhesion on mechanical characteristics of the single chondrocyte,” Journal of orthopaedic research, vol. 21, no. 1, pp. 88-95, 2003.

[77] U. Dammer, O. Popescu, P. Wagner, D. Anselmetti, H. J. Guntherodt, and G. N. Misevic, “Binding strength between cell adhesion proteoglycans measured by atomic force microscopy,” Science, vol. 267, no. 5201, pp.1173-1175, 1995.

[78] K. A. Addae-Mensah, and J. P. Wikswo, “Measurement techniques for cellular biomechanics in vitro,” in Experimental biology and medicine, vol. 233, no. 7, pp. 792-809, 2008.

[79] G. Fu, C. Milburn, S. Mwenifumbo, Y. Cao, G. M. Oparinde, M. O. Adeoye, and W. O. Soboyejo, “Shear assay measurements of cell adhesion on biomaterials surfaces,” Materials Science and Engineering: C, vol. 29, no. 4, pp. 1293-1301, 2009.

[80] R. Salánki, C. Hős, N. Orgovan, B. Péter, N. Sándor, Z. Bajtay, A. Erdei, R. Horvath, B. Szabó, “Single Cell Adhesion Assay Using Computer Controlled Micropipette,” PloS one, vol. 9, no. 10, 2014.

[81] I. Z. Veronika, & and Z. Cheng, “Adhesion Frequency Assay for< em> In Situ Kinetics Analysis of Cross-Junctional Molecular Interactions at the Cell-Cell Interface,” Journal of Visualized Experiments, vol. 57, 2011.

[82] D. Navajas, F. Rico, P. Roca-Cusachs, N. Gavara, R. Farré, M. Rotger, “Probing mechanical properties of living cells by atomic force microscopy with blunted pyramidal cantilever tips,” Physical Review E, vol. 72, no. 2, 021914, 2005.

[84] M. Radmacher, M. Fritz, C. M. Kacher, J. P. Cleveland, P. K. Hansma, “Measuring the viscoelastic properties of human platelets with the atomic force microscope,” Biophys J, vol. 70, pp. 556–567, 1996.

[85] M. Radmacher, R. W. Tillmann, H. E. Gaub, “Imaging viscoelasticity by force modulation with the atomic force microscope,” Biophys J, vol. 64, pp. :735-742, 1993.

[86] E. Ruoslahti, J. C. Reed, “Anchorage dependence, integrins, and apoptosis, Cell, vol. 77, no. 4, pp. 477–478, 1994.

[87] Balaban, Q. Nathalie, et al., “Force and focal adhesion assembly: a close relationship studied using elastic micropatterned substrates,” Nature cell biology, vol. 3, no. 5, pp. 466-472, 2001.

[88] RJ. Pelham, Y. Wang, “Cell locomotion and focal adhesions are regulated by substrate flexibility,” Proc Natl Acad Sci USA, vol. 94, no. 25, pp. 13661–12665, 1997.

[89] S. Usami, H.H. Chen, Y. Zhao, S. Chien, R. Skalak, “Design and construction of a linear shear stress flow chamber,”Annals of Biomedical Engineering, vol. 21, no. 1, pp. 77–83, 1993.

[90] V.A. Resto, M.M. Burdick, N.M. Dagia, S.D. McCammon, S.M. Fennewald, R. Sackstein, “L-selectin-mediated lymphocyte-cancer cell interactions under low fluid shear conditions,”Journal of Biological Chemistry, vol. 283, pp. 15816–15824, 2008.

3.0 CHAPTER THREE: METHODOLOGY

3.1 Introduction

This chapter presents the experimental procedures that were used for: the fabrication of Poly (dimethylsiloxane) (PDMS) substrates; the various methods used for the surface modification of PDMS; surface chemistry used to ascertain the chemical changes that occurred on modified PDMS. SEM analysis was done to view to surface morphology of unmodified and modified PDMS substrates. Also, the mechanical test that was used to determine the stiffness of different mix ratios and curing temperatures of PDMS are presented.

3.2 Materials and Methods

The apparatus that were used in the PDMS fabrication includes: petri dish, syringes, glass slides, GALVAC vacuum oven (LTE Scientific LTD., Greenfield); for chemical modification of PDMS substrates, Digital UV Ozone System (Figure 3.1 D), hot plate, beakers, and distilled water. IR Affinity Fourier Transform Infrared (FTIR) Spectrometer (Figure 3.1 C) was used for surface chemical assay. Also, slygard elastomer kit (Figure 3.1 B), purchased from Dow Corning Corporation, Midland, MI 48686-0994, USA was used for PDMS synthesis.

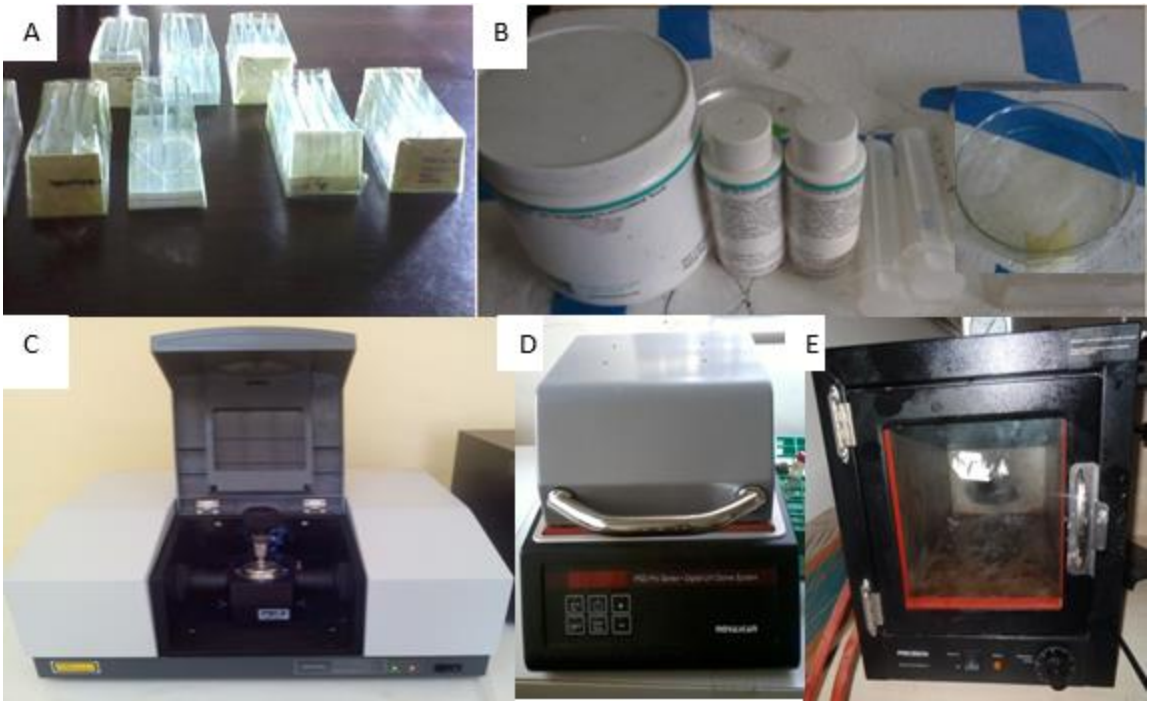

Figure 3.1: Chemicals and apparatus used in PDMS preparation (A) molds for PDMS samples for mechanical test, (B) Slygard elastomer kit, syringes and petri dish, (C) FTIR Spectrometer, (D) Digital UV Ozone System, (E) GALVAC vacuum oven

3.3 Experimental Procedures

3.3.1 Fabrication

To investigate the material property (stiffness) of Sylgard 184, multiwall moulds were made in accordance to dimensions required by the Instron Senohydraulic Testing Machine (Model 3360, Norwood, Massachusetts, USA). The moulds were made from glass slides as shown in Figure 3.1A.

3.3.2 Preparation of PDMS

All experiments were performed with Sylgard-184, an elastomeric PDMS kit manufactured by Dow Corning. The components for preparing the elastomers were supplied in two parts, Sylgard-184A and Sylgard-184B. PDMS was prepared by mixing

the sylgard silicon elastomer base (A) to curing agent (B) in a 10:1 volume ratio. The mixture was stirred vigorously in a petri dish and de-gassed with a GALVAC vacuum oven (LTE Scientific LTD., Greenfield) at -25 in Hg with no heat for an hour. This was to ensure that bubbles or entrapped gases were adequately removed. PDMS was then cast into the moulds and then cured in vacuum oven. Rectangular samples of equal dimensions of 5 mm x 5 mm x 75 mm were made for mechanical testing (as shown in Fig. 3.2).The samples were formed at different mix ratios and curing temperature as summarized in table 3.1. For other measurements, the PDMS substrates were prepared by casting the Sylgard-184A/Sylgard-184B mixtures into a flat glass Petri dish and cured at 60˚C for 12 hours. The cured PDMS substrates (~0.5 mm thick) were then cut into 10×10 mm squares. The substrates were enclosed in a petri dish to prevent contamination before use.

Table 3.1: Summary of mix ratio and curing temperature of PDMS

Mix ratio of sample	Curing temperature (^{o}C)		
10:1	50	100	150
50:1	50	100	150
100:1	50	100	150

Figure 3.2: PDMS samples of sizes (5 mm x 5 mm x 75 mm) for mechanical testing

The optical transparency of cured PDMS enabled all samples to undergo a visual inspection to identify possible tears, bubbles or other visually detectible defects that could affect the mechanical integrity of the samples. With the exception of 100:1 mix ratio, the others did not have tears.

3.3.3 Surface Modification of PDMS

The surfaces of PDMS samples were modified via various methods to become more cells friendly. The methods employed in this work are UVO treatment, boiling water technique, and Coating with poly (lactic-co-glycolic acid) (PLGA).

PLGA was considered for coating because it belongs to a family of FDA-approved biodegradable polymers that are physically strong and highly biocompatible and have been extensively studied as delivery vehicles for drugs [1]. It was used in this work to observe any possible modification that could be introduced on the PDMS.

3.3.3.1 UV/Ozone Treatment

The UVO treatment of the PDMS surface was carried out in a Digital UVO chamber (PSD Pro Series, novascan). The PDMS substrate was placed on the UVO sample stage at a distance of about 5mm from the UV source. The samples were incubated (with the power off) in the ozone environment for 30 minutes. This was to allow ozone to attack the sample. Following this, the controller was programmed at a temperature of 25◦C with time set at 30mins. The start button is pressed and cleaning of the sample initiates until the time exposure reached. On completion, the equipment was turned off and the samples removed after 30 mins and kept in petri dish.

3.3.3.2 Boiling water treatment

Following the PDMS elastomer preparation previously described, it was degassed and cured in a vacuum oven for 11 h at 60 ◦ C, followed by room temperature cooling for 3 h. PDMS samples (1mm thick, 100mm^2) were immersed in a beaker of boiling deionized (DI) water for 0.5, 1, 1.5, and 2 h, then quickly removed and blotted dry on a wipe prior to analysis.

3.3.3.1 UVO Treatment

The UVO treatment of the PDMS surface was carried out in a Digital UVO chamber (PSD Pro Series, novascan). The PDMS substrate was placed on the UVO sample stage at a distance of about 5mm from the UV source. The samples were incubated (with the power off) in the ozone environment for 30 minutes. This was to allow ozone to attack the sample with much ozone dissipated. Following this, the controller was programmed at a temperature of 25˚C with time set at 30mins. The start button was pressed and cleaning

of the sample initiated until the time exposure reached. On completion, the equipment was turned off and the samples removed after 30 mins and kept in petri dish prior to surface chemistry assay.

3.3.3.2 Boiling water treatment

Following the PDMS elastomer preparation previously described, it was degassed an cured in a vacuum oven for 11 h at 65 ◦ C, followed by room temperature cooling for 3 h. PDMS samples (1mm thick, 100mm^2) were immersed in a beaker of boiling water for 0.5, 1, 1.5, and 2 h, then quickly removed and blotted dry on a wipe prior to analysis..

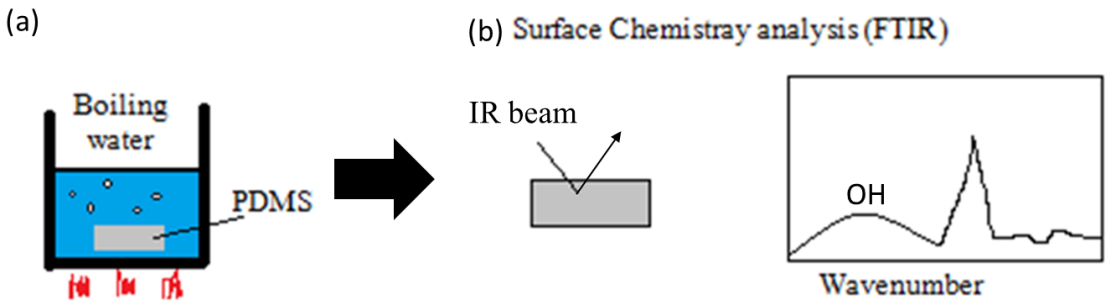

Figure 3.3: Schematic of (a) PDMS modification by boiling water, (b) surface chemistry analysis

The theory involved in the generation of the OH group on PDMS substrate is as follows: PDMS is cured by an organometallic crosslinking reaction [2]. The constituent of PDMS are siloxane base oligomers (containing vinyl groups) and curing agent (containing a proprietary platinum-based) [2]. The crosslinking is typically by the Pt-catalyzed

hydrosilylation reaction to form a flexible elastomer [3]. The curing reaction of PDMS involves the Pt-catalyzed hydrosilylation of vinyl-terminated PDMS and vinylated silica (their combination represented generically as PDMS-Vi) with an oligomeric siloxane (PDMS-H) multifunctional in silicon hydride (SiH) groups to form an end-linked network of PDMS (Figure 3.4).

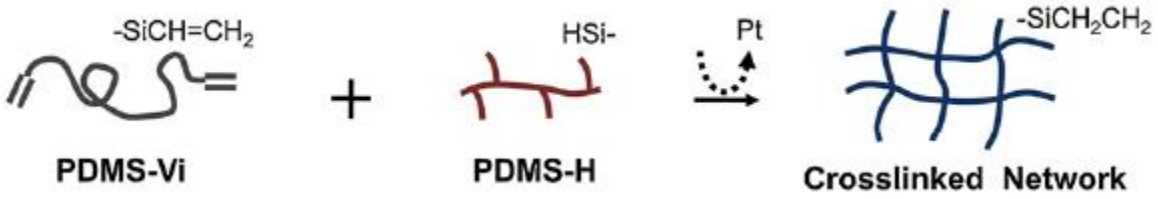

Figure 3.4: Schematic hydrosilylation crosslinking reaction used to cure SYLGARD® 184 PDMS elastomer [3].

The presence of excess SiH groups in the cured PDMS, results in the proposed hypothesis reaction which occurs near the PDMS elastomer surface in boiling water:

$$(\text{-SiH}) + H_2O \xrightarrow{Pt} (\text{-Si-OH}) + H_2\uparrow \quad \text{.....Equation 1[4]}$$

This reaction as previously discussed in chapter 2 makes the substrate polar and hence cell – friendly.

3.3.3.3 Coating with PLGA

PLGA was deposited onto PDMS by spin coating process. This was done using a 400 Lite spinner (Laurell Technologies, North Wales, PA) at 1000 revolutions per minute (rpm).

3.3.4 Surface Chemistry Assay

To characterize the chemical changes that took place on the surface of PDMS, Fourier Transform Infrared (FTIR) analysis was employed. This was done using an IR Affinity FTIR Spectrophometer. 10 scans were collected for each sample with a resolution of 4 cm−1 under constant nitrogen flux to eliminate the effect of water vapor on the collected data. The data was collected in the range of 4000–500 cm^{-1}.

3.3.5 Topographical Analysis of PDMS

SEM images were taken to analyze the topography of PDMS. Images of unmodified, UVO treated and PLGA coated were taken and compared to observe the differences in topography.

3.4 Reference for Chapter three

[1] H. K. Makadia and S. J. Siegel, "Poly Lactic-co-Glycolic Acid (PLGA) as Biodegradable Controlled Drug Delivery Carrier," Polymer 3.3, pp: 1377-1397, 2011.

[2] D. J. Campbell, K. J. Beckman, C. E. Calderon, P. W. Doolan, R. H. Moore, A. B. Ellis, G. C. Lisensky, "Replication and Compression of Bulk Surface Structures with Polydimethylsiloxane Elastomer," in Uses of Polydimethylsiloxane (PDMS) Elastomer, J. Chem. Educ. Vol. 76, p. 537, 1999.

[3] J. Yull, D. Ahn, Y. Young, C. Mo, S. Takayama, S. Hyuck, and S. Lee, "Surface chemistry modification of PDMS elastomers with boiling water improves cellular adhesion," *Elseveier Sensors & Actuators B: Chemical*, vol. 173, pp. 765–771, 2012.

[4] M.A. Brook, “Silicon in Organic, Organometallic, and Polymer Chemistry,” J. Wiley, New York, p. xxiv, 680, 2000.

4.0 CHAPTER FOUR: MODELLING

4.1 Introduction

This chapter presents analytical and computational model approach used to study Au/PDMS buckling systems and shear assay. Au/PDMS system was studied analytically by calculating the stresses required to cause buckling by coating Au on PDMS. This was done at different pre-strain values. The bucking profiles of Au/PDMS was also observed by computational models. Also, the effects of pre-strain, and substrate modulus on wavelength of buckle profile was analyzed and compared to experimental result. To study the effects of surface modification on cell adhesion, shear assay model was used.

4.2 Analytical Modelling

Coating of thin metal films on elastomeric substrates results in ordered buckling structures [1]. The compression induced buckling instability of the thin film resulting in surface buckling of the thin film which may also lead to fracture and delamination [2]. In the context of interfacial fracture mechanics, the buckling profiles can be analyzed.

The driving force for crack growth can be defined in terms of the elastic strain energy release rate, G. There has been analytical calculation of the energy release rate, G , of the interfacial crack in buckle-driven delaminated thin film from a substrate [3]. This is presented in equation 1:

$$G = \left[(1-\nu_f^2)h/(2E_f)\right](\sigma_R - \sigma_c)(\sigma_R + 3\sigma_c) \quad \text{.....Equation 2}$$

Where E_f, ν_f and *h* are the Young's Modulus, Poisson's ratio and thickness of Au film respectively; σ_R is the residual stress in the Au film and σ_c is the critical buckling stress.

It has been shown in literature that the residual stress is directly proportional to the amplitude of buckling: an increase in amplitude of the buckling results in increase residual stress [4]. This causes delamination to initiate. Therefore, the thin film starts to delaminate from the substrate when residual stress exceeds the critical stress for buckling. From this, the interfacial energy release rate, G, is expected to approach a critical value, G_c. This critical value is presented in equation 2.

$$G_c = \left[\left(1-\nu_f^2\right)h/2E_f\right]\sigma_f^2 \quad \text{..... Equation 3}$$

From equation 1, it is important to determine the residual stress, σ_R in the film and the critical buckling stress, σ_c. This is because buckled structures are formed as a result of induced residual stress on the film.

As temperature drops to room temperature after film deposition, buckling initiates when maximum principal compressive stress attains the critical value. Below this critical stress level, no buckling initiates within the Au film. For buckling of a film on a polymer layer, the critical stress, equation 4 presents a solution to the calculation o of the critical stress, for the onset buckling of thin films [7].

$$\sigma_c \approx 0.52\left[E_f/\left(1-\nu_f^2\right)\right]^{1/3}\left[E_s/\left(1-\nu_s^2\right)\right]^{2/3} \quad \text{.....Equation 4}$$

Where E_f and E_s are the Young's moduli of the film and the substrate, ν_f and ν_s are the Poisson ratios of the film and the substrate. The critical stress has been expressed as a function of wavelength of the buckling as presented in equation 4 [7]. This is given by:

$$\sigma_c = \pi^2 h^2 E_f / 3\lambda^2 \left(1-\nu_f^2\right) \text{ .....Equation 5}$$

Where λ is the wavelength of the buckle profile and other parameter have their usual meaning as previously defined.

4.2.1 Residual and Applied Stresses

The formation of buckling for applications in biomedical devices for cell contact guidance involves deposition of a thin film onto pre-stretched substrate [8]. There is thermal expansion coefficient mismatch between the film and the substrate during coating. This subjects the film to stress. Also by pre-stretching the substrate the film is subjected to stress. Buckling occurs as a results of these stresses. The residual stress, σ_{th}, as a results of thermal expansion coefficient mismatch is presented in equation 5 [7]:

$$\sigma_{th} = \left[E_f(\alpha_f - \alpha_s)(T_d - T)\right]/\left(1-\nu_f\right) \text{.....Equation 6}$$

where E_f and ν_f are Young's modulus and Poisson's ratio of the film; α_f and α_s are the thermal expansion coefficients of the film and the substrate respectively ; T_d is the deposition temperature and T corresponds to the room temperature. The stress, σ_{app}, due to the release of the applied pre-stretched substrate can be approximated as:

$\sigma_{app} = E_f \varepsilon_{pre}$ ..... Equation 7

where ε_{pre} corresponds to the pre-strain. By applying the principle of linear superposition, the total residual stress in the film can be expressed from Equations (5) and (6). This is given by:

$\sigma_R = \sigma_{th} + \sigma_{app} = \left[E_f (\alpha_f - \alpha_s)(T_d - T)\right] / \left(1 - \nu_f\right) + E_f \varepsilon_{pre}$ Equation8

The amount of residual stress responsible for wrinkling and delamination-induced buckling in the thin film deposited onto pre-stretched polymeric substrate is presented in equation 7.

4.3 Computational Modelling

4.3.1 Au/PDMS Buckling Model

Finite element analysis of Au/PDMS buckling and ECM/PDMS buckling system were performed. The finite element analysis consists of 0.01mm thick PDMS substrate and a 100nm thick Au film , with a 1mm length of the two dimensional system. The modelling was done in ABAQUS™ software package (ABAQUS 6.12-1, Dassault Systems Incoporation, SA). The stress-free thin film is attached to the pre stretched substrate by sharing the same nodes at the thin film/substrate interface. The rotational degree of freedom in the substrate elements was constrained. 2D-Axis Symmetry model 4-node bilinear plane stress quadrilateral was used. Very fine mesh, with the smallest element size of (0.2), near the film/substrate interface was used to ensure that the results converge and also to overcome the difficulties of the analysis. The type of element used was quad. The ends of the film-PDMS model were displaced with different residual compressive

strain (0.18, 0.36, and 0.70) to observe its effects on the buckling profile. The modulus of the PDMS substrate used for the simulation were (1.46, 2.07, and 2.35 MPa) as obtained from experimental work of a 10:1 mix ratio and cured 50, 100, and 150˚C respectively, with Poisson ratio of 0.48 [6,7]. Poisson ratio of 0.33 was also used for Au. This was to study the effects of substrate modulus on the buckling profile.

4.3.2 Shear Assay Model

The flow field, in which cells are detached from the substrate, was built to model the conditions in the shear assay chamber (Fig 2.8 a). The cell and substrate properties that was used is presented in table 4.1. Axis symmetry grid geometry model was used. The element type was 4-node bilinear plane stress quadrilateral. The model incorporated an initial cell model that was built from two-dimensional image of typical undeformed cells. The cell was put on a PDMS substrate. The thickness of PDMS and silica layer were 0.01mm and 100nm respectively. An interfacial crack of length 1μm was introduced between the cell and the substrate. Shear and lift loads were applied to observe its effects on crack opening. The shear and lift force were 1e-5Pa and 1e-6Pa respectively. The energy release rate associated with crack opening was used to determine the effect of surface modification on cell adhesion.

Table 4:1: Materials properties incorporated in model

Materials	**Mechanical Property**	
	Young's Modulus (MPa)	Poisson Ratio
Cell cytoplasm	530	0.5
Nucleus	300	0.49
PDM	(1.46, 2.07, 2.35)	0.48
Silica Film	70	0.3

4.4 Reference for chapter four

[1] N. Bowden, S. Brittain, A.G. Evans, J.W. Hutchinson, G.M. Whitesides, "Spontaneous Formation of ordered structures in thin films of metals supported on an elastomeric polymer," Nature, vol. 393, (6681), pp. 146-149, 1998.

[2] H. Mei and R. Huang, "Wrinkling and Delamination of Thin Films on Compliant Substrates," 13th International Conference on Fracture, June 16–21, Beijing, China, 2013.

[3] J. W. Hutchinson, and Z. Suo. "Mixed mode cracking in layered materials," Advances in applied mechanics, vol. 29, pp. 63-191, 1991.

[4] Y. Ebata, A. B. Croll and A. J. Crosby, "Wrinkling and strain localizations in polymer thin films," Soft Matter, vol. 8, pp. 9086-9091, 2012.

[5] D. H. Kim, et al., "Stretchable, curvilinear electronics based on inorganic materials," Advanced Materials, vol. 22, no.19, pp. 2108-2124, 2010.

[6] Xu, Hao, and Keji Chen, “Integrative medicine: the experience from China,” The Journal of Alternative and Complementary Medicine, vol.14, no. 1, pp. 3-7, 2008.

[7] O. Akogwu, D. Kwabi, A. Munhutu, T. Tong, and W. O. Soboyejo, “Adhesion and cyclic stretching of Au thin film on poly (dimethyl-siloxane) for stretchable electronics,” J. Appl. Phys., vol. 108, no. 12, 123509, 2010.

5.0 CHAPTER FIVE: RESULTS AND DISCUSSION

5.1 Introduction

The chapter presents results and discussion of experimental methods from chapter 3 and analytical and computational results of chapter five.

As previously discussed, mechanical properties were tested for samples cured at temperatures of 50 ◦C, 100 ◦C, and 150 ◦C. In total 24 PDMS test pieces were used for mechanical experimental testing.

5.2 Tensile

The influence of mix ratio and curing temperature on the tensile strength of Sylgard 184 PDMS was determined by averaging the data from each of three test samples for every curing temperature. The Young's modulus of the PDMS samples for each curing temperature was calculated for the linear elastic region (<40% strain) using Hooke's law. The stress-strain curve of PDMS is nonlinear; hence the secant modulus (Fig. 5.1) was used to determine the young's modulus.

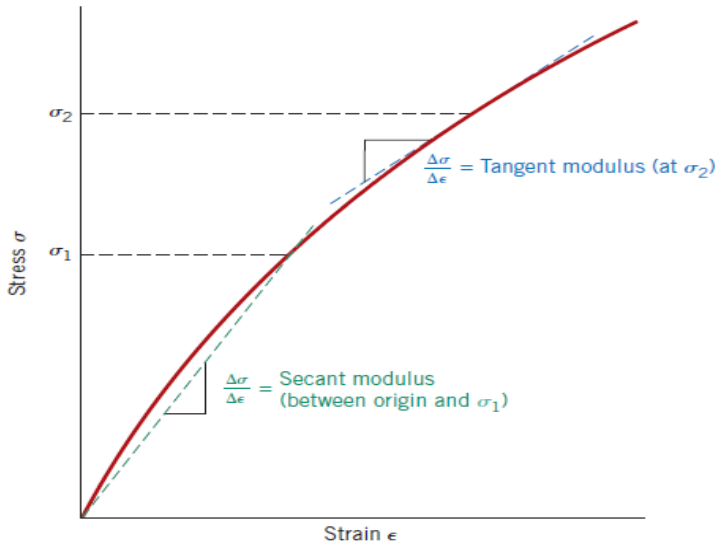

Figure 5.1: Schematic stress–strain diagram showing non-linear elastic behavior and tangent modulus is determined [1].

The load – extension curve for one batch of samples (10:1 cured at 150^{o}C) as obtained from the Instron Senohydraulic Testing Machine is showed in Fig. 5.2

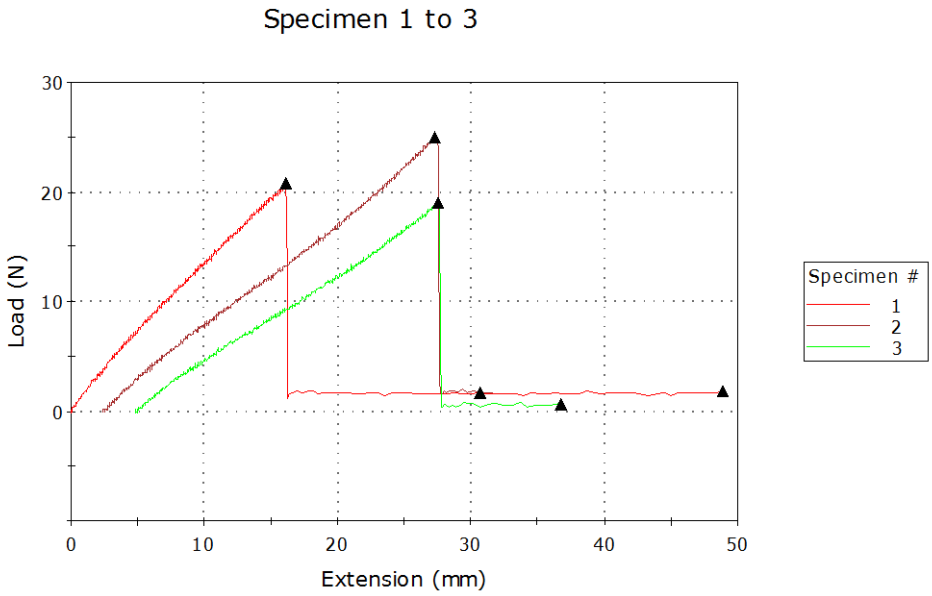

Figure 5.2: The load – extension curve of 10:1 samples cured at 150^{o}C.

From the load-extension curve in Fig 5.2, the stress was obtained by dividing the load with the area of the sample. The strain was also obtained from the extension using the original length of the sample. With this, the secant modulus was calculated and the results are presented in table 5.1. Each young's modulus presented is an average of 3 samples. The samples mixed at 100:1 ratio did not gave inconclusive results; on curing at various temperatures (up to 200^{o}C), they still were not well cured.

The following equations were used in the determination on the young's modulus of PDMS.

$$Stress, \sigma = \frac{Applied\ load\ (normal\ to\ surface)}{Cross\ sectional\ area}$$ **.....Equation 1**

The strain was calculated from the extension as:

$$Strain, \varepsilon = \frac{Extension}{Original\ length\ of\ PDMS}$$ **.....Equation 9**

The modulus was then calculated using equation:

$$stress, \sigma = modulus, E \times straian, \varepsilon$$ **.....Equation 10**

From equation 3, young's modulus is calculated as:

$$E = \frac{Stress}{Strain}$$ **..... Equation 11**

Table 5.1: Results of young's modulus of PDMS samples of different mix ratios and curing temperatures.

Mix ratio of sample	Curing Temperature (^{o}C)	Young's Modulus (MPa)
10:1	50	1.46±0.073
	100	2.07±0.1035
	150	2.35±0.1175
50:1	50	0.13±0.0065
	100	0.17±0.0085
	150	0.19±0.0095

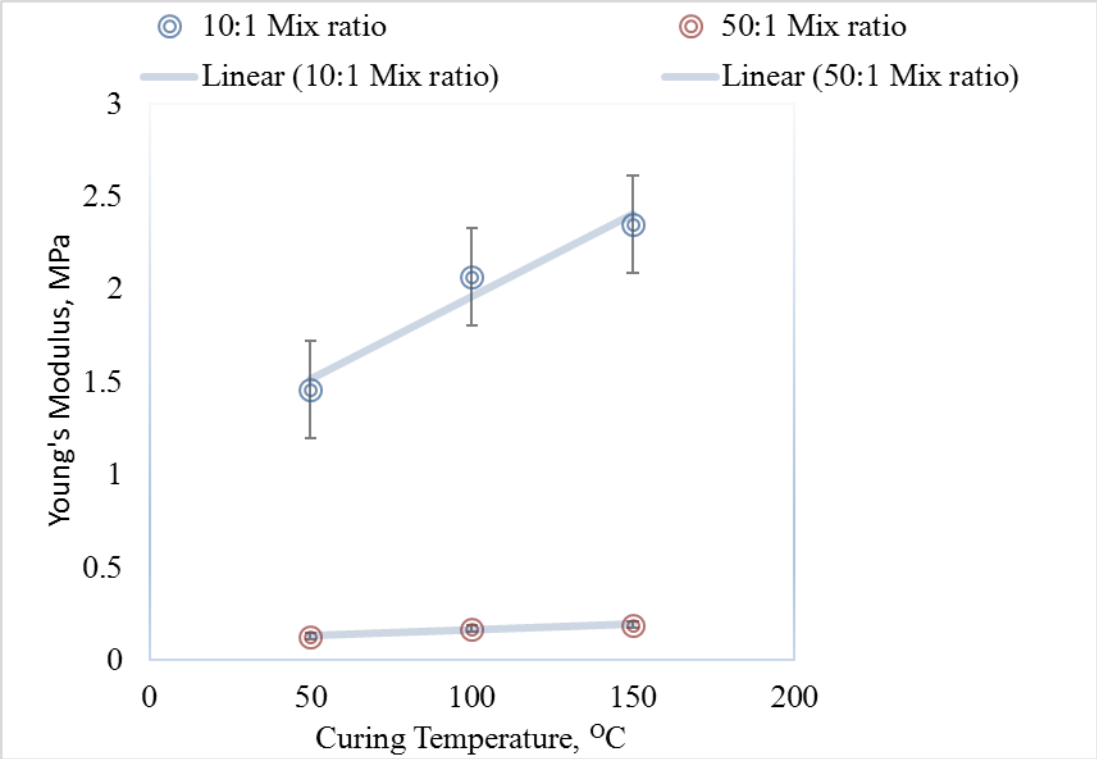

Figure 5.3: Relationship between curing temperature of PDMS and the resultant Young's modulus at different mix ratios

The graph in Fig 5.3 shows an increase in young's modulus with increasing curing temperature for both mix ratios. The young's modulus of the 10:1 mix ratio was higher than that of 50:1 at all curing temperatures. It was found that the Young's modulus of the samples undergoing tensile testing was linearly dependent on their curing temperature within the temperature range investigated. Also, increasing the sylgard base decreases the modulus of PDMS.

The increase in modulus of PDMS with curing temperature could be attributed to the crosslinking reaction. The siloxane base oligomers contain vinyl groups, with at least 3 silicon hydride bonds each in the cross-linking oligomers [2]. The proprietary platinum-based catalyst contained in the curing agent catalyzes the addition of the SiH bond across the vinyl groups, forming Si-CH_2-CH_2-Si linkages. This multiple reaction sites on both the base and crosslinking oligomers allow for three-dimensional crosslinking [2].

Lower degree of PDMS network's crosslinking results in lower stiffness (smaller modulus) [3]. A higher degree of PDMS network's crosslinking will therefore imply a stiffer sample (greater modulus). Heating is also known to accelerate the crosslinking reaction [1]. From this reasoning it can be inferred that, increasing the curing temperature led to a higher degree of PDMS network's crosslinking, and subsequently increased the modulus.

In an unstressed state PDMS is amorphous and composed of cross-linked chains that are twisted, kinked, and coiled. During tensile loading, there is partial uncoiling,

untwisting, and straightening, and the resultant elongation of the chains in the stress direction [1]. This phenomenon presented in Figure 5.4

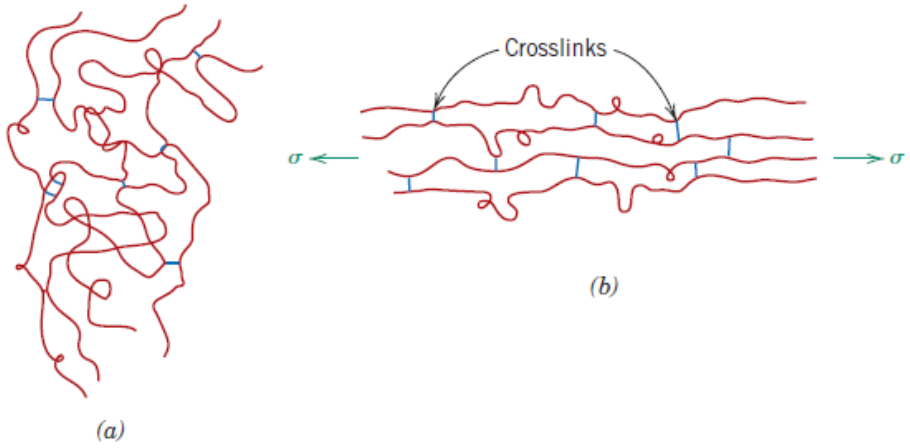

Figure 5.4: Schematic presentation of cross-linked polymer chain molecules (a) in an unstressed state and (b) during elastic deformation in response to an applied tensile stress [1]

From figure 5.4, it is deduced that heavily cross-linked PDMS will have more resistance to deformation (partial uncoiling, untwisting, and straightening). Since increasing curing temperature results in more cross-linked PDMS, upon application of tensile load, resistance to deformation will be high. This also explains the increase in tensile modulus with increasing temperature.

The modulus observed for the mix ratio 10:1 was (1.46, 2.07, and 2.35) and that of 50:1 was (0.13, 0.17, and 0.19). This observation could be as a result of the effect of curing agent to base on crosslinking. It has been reported that as the ratio of curing agent to base is increased, a harder, more cross-linked elastomer results [2]. Ratio 10:1 implies more curing agent as compared to 50:1. Therefore ratio 10:1 is expected to form cross-linked PDMS, hence the higher modulus.

5.3 FTIR Results

FTIR measurement was used to elucidate information about chemical functionality groups present in untreated PDMS and PDMS samples treated via boiling water and UVO. In Fig 5.5 FTIR spectra is plotted for untreated PDMS (control) and boiled PDMS samples at different times: 30 mins, 60 mins, 90 mins, and 120 mins. Fig 5.6 also show FTIR spectra for PDMS sample treated via UVO for 30 mins and 1hour. PDMS exhibits several characteristic IR bands in table 5.2. The most intense peaks in FTIR spectra are associated with $–CH_3$ rocking and ≡Si–C≡ stretching (peak 8), ≡Si–OH stretching (peak 6, 7), asymmetric Si–O–Si stretches (peak in 4), symmetric –CH3 deformations (peak 3), asymmetric $Si–CH_3$ stretches (peak 2), and asymmetric Si–OH stretches (peak 1).

Table 5.2: Assignment of IR Spectra of PDMS [4]

Peak in FTIR spectra	IR Region	Description
1	3200-3600	–OH stretching in ≡Si–OH
2	2950-2970	Asymmetric $–CH_3$ stretching in ≡Si.CH_3
3	1245–1270	Symmetric $–CH_3$ deformation in ≡Si–CH_3
4	1055–1090	Asymmetric ≡Si–O–Si≡ stretching in $[–(CH_2)_2Si–O–]_x$
5	1000-1050	In-phase and out-of-phase wagging vibrations of $–(CH_2)–$ in ≡Si–$(CH_2)_2$–Si≡ and ≡Si–CH2–Si≡
6	875-900	≡Si–O stretching in ≡Si–OH
7	825-865	≡Si–O stretching in ≡Si–OH
8	785–815	$–CH_3$ rocking and ≡Si–C≡ stretching in ≡Si–CH_3

From a visual inspection of the FTIR spectra in Fig 5.5, it is seen that there is an increase in –OH signal (peak 1) with increasing boiling time. This occurred with a simultaneous decrease in the band intensity characteristic of the Si–O–Si signal (peak 4). The occurrence of this is an indication of chain scission in the PDMS network [4]. There was also a slight decrease in peak 8 (–CH3 signal). The decrease in $–CH_3$, along with increase in –OH signal implies a possibility of PDMS becoming hydrophilic as a result of oxidative conversion of $–[(CH_3)_2Si–O] –$. As observed in Fig 5.5, the OH peak increases with increasing boiling time. This suggest that boiling for a longer period could result in a more hydrophilic PDMS substrate. In this work the evidence of SiOH group from the FTIR analysis was at 3400 cm^{-1}, with the highest absorbance at 0.025 for PDMS samples boiled for 120 mins.

When exposed to boiling water, changes occurs in the surface of the PDMS as a result of chain scission which leads to the formation of hydroxyl (OH) group. During chain scission, breaking of molecular bonds occurs and allows atoms to react with themselves [5]. This could lead to the formation of SiH. This SiH the reacts with the water to form SiOH presented in the reaction below [6]:

$$(\text{-SiH}) + H_2O \xrightarrow{Pt} (\text{-Si-OH}) + H_2\uparrow.$$

In the reaction the proprietary platinum in the curing agent acts as a catalyst for the chemical conversion.

The vinyl functional silica filler present in the SYLGARD® 184, could also result in residual SiOH groups on the surface of PDMS. Although the silica present is vinyl functionalized to minimize mobility after crosslinking, any silica near the surface may be

susceptible to localized surface reorientation of the PDMS network to bring any hydrophilic SiOH groups to the surface [7].

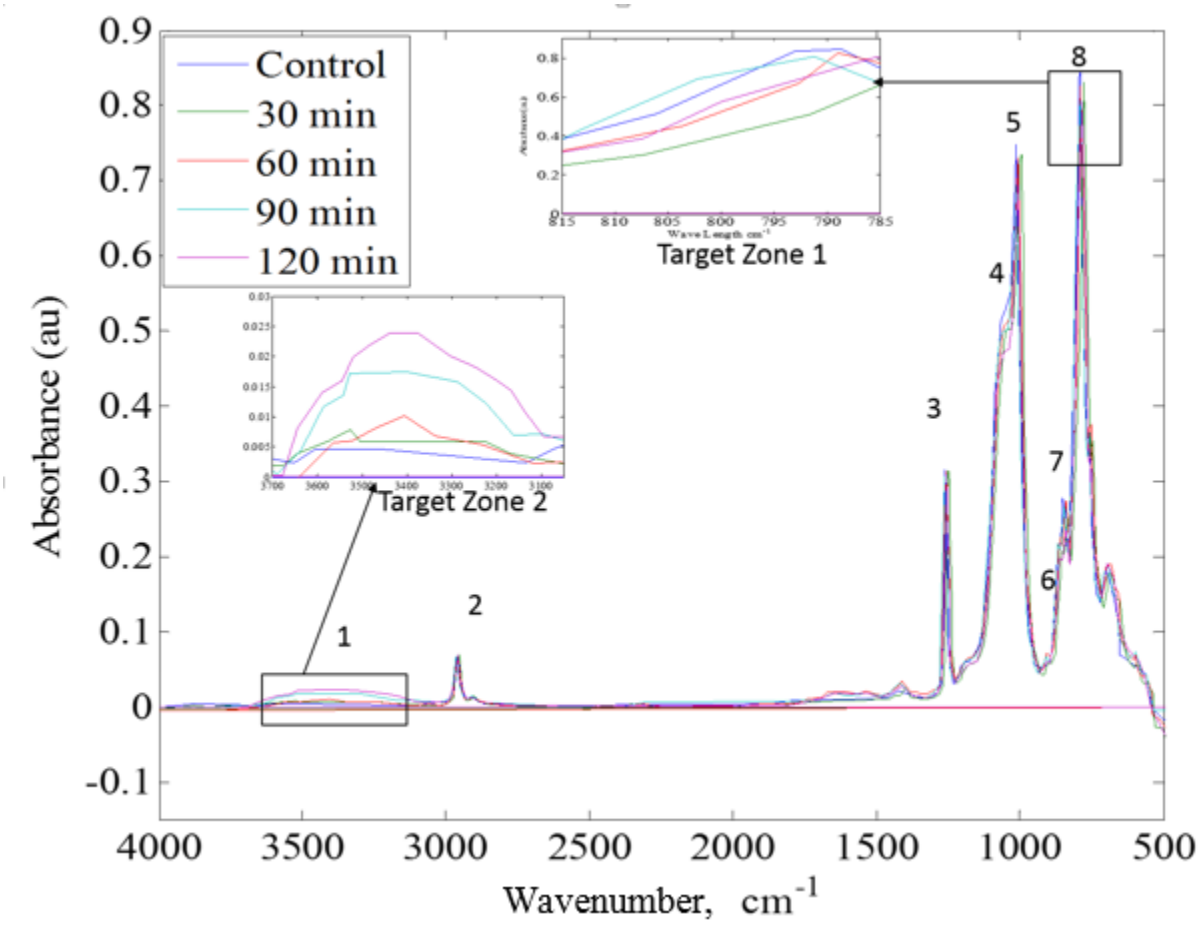

Figure 5.5: Graph showing overlays of infrared (IR) spectra from the untreated PDMS (control) and treated PDMS substrates via boiling water at different times: Target Zone 1 shows a decrease in $–CH_3$ peak and target zone 2 showing an increase in OH peak

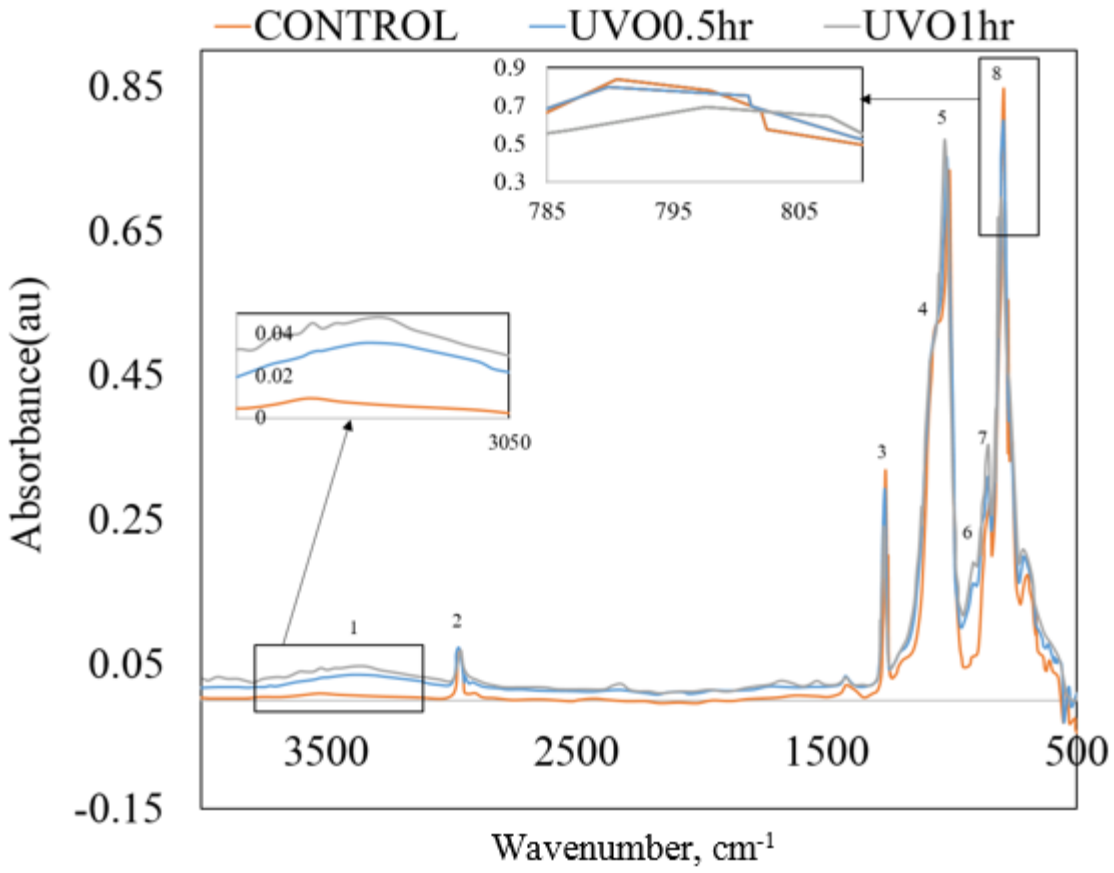

Figure 5.6: Graph showing overlays of infrared (IR) spectra from the untreated (control) and treated PDMS substrates via UVO for 30 mins (UVO0.5hr) and 60mins (UVO1hr).

From Fig 5.6, a similar observation is made as in Fig 5.5. The decrease in peaks 3 and 8 (–CH_3 signal), with an increase in peak 1 (OH signal) is an indicative of oxidative conversion as previously discussed. The highest OH peak is observed at absorbance (~0.035) for PDMS samples treated for 60 mins.

In UVO treatment, there is photosensitized oxidation process in which the molecules of the treated material are excited by absorption of short wavelength UV radiation in a range λ=185-254 [4]. The UVO treatment generates atomic oxygen in a combination of photochemical processes. The ozone is produced from the 185nm line from molecular

oxygen, and it is converted to atomic oxygen by the 254nm ozone line. For the treatment of PDMS, the siloxane backbone of PDMS is attacked by this oxygen species to form oxygen rich silica-like (SiO_X) layer and Si-OH surface. The formation of the Si-OH surface is a possible reason for the generation of OH peak in Fig 5.6. The increase in OH peak with treatment suggests that as time increases, the concentrations of ozone and atomic oxygen increases leading to large number of hydrophilic functionalities.

5.3 SEM Result

The SEM images revealed some physical changes on the surface of treated PDMS. The images are presented in Figure 5.7

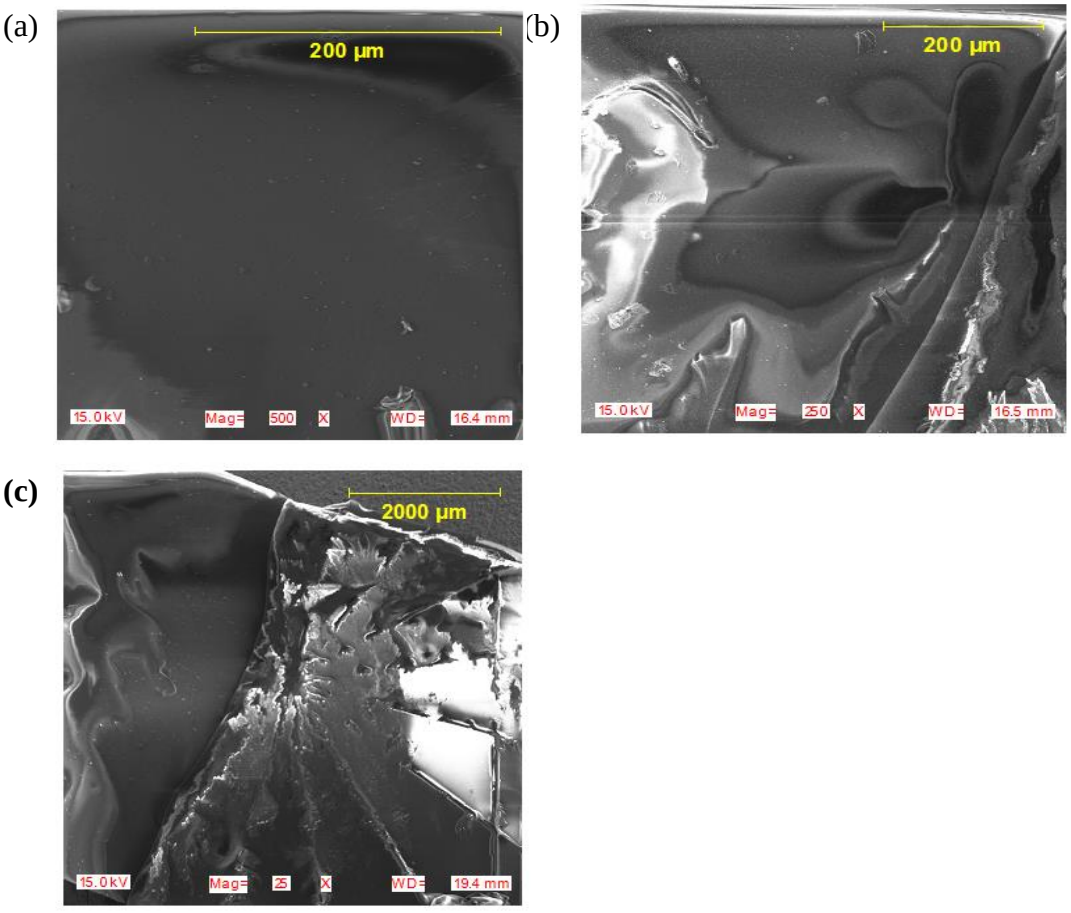

Figure 5.7: SEM images of (a) untreated PDMS, (b) PDMS sample treated via UV ozone, (c) PDMS coated with PLGA

From figure 5.7 a, it is observed that the surface of PDMS is plain. There appears to be a layer formed on the PDMS substrate (Fig 5.7 b). This could possibly be the silica-like layer formed upon the attack by UVO. Coating PDMS with PLGA revealed some texture surface. The topology of the modified PDMS has the tendency to enhance cell adhesion and growth.

5.4 Analytical Model Results

5.4.1 Stress Analysis of Analytical Model

There is residual stress in Au film as a result of thermal expansion coefficient mismatch between the film and substrate, when Au is deposited on pre-stretched PDMS. Akogwu et al., have reported the average textured Young's Modulus for the Au film ~61 GPa, and deposition temperature to be ~50˚C [7]. By incorporating the measured modulus of the Au film into Equation (6) along with the temperature difference of 295K (assuming room temperature to be 28˚C), Poison ratio (υf =0.33) and thermal expansion coefficients of the Au-film ($\alpha f = 1.4 \times 10^{-5}$) and substrate ($\alpha s$=$3.14 \times 10^{-4}$), the residual stress due to thermal expansion mismatch was calculated to be - 8.057GPa. The stress due to the pre-strained PDMS substrate (0.18, 0.36, and 0.70) was calculated from Equation (7), with the results presented in table 5.2. By combining the thermal and applied residual stress in equation 8, the residual stress is obtained. The calculated residual stress increases with increasing pre-strain of the PDMS substrate.

The critical stresses required for buckling to occur was also calculated for PDMS substrate modulus in a range of 1-100MPa. This was then used to predict the limiting critical stress for the Au thin film on a specific PDMS substrate (of known modulus: 1.46, 2.07, 2.35 MPa).For example, in Figure 5.4, the critical stresses of Au film on PDMS substrates of moduli 1.46 MPa and 2.35 MPa are 0.000142 GPa and 0.00032 GPa respectively. Critical stress increases with increasing substrate modulus.

Table 5.3: Residual stresses due to effects of thermal expansion coefficient mismatch and pre-strained PDMS substrate.

Pre-strain	**Applied Stress**	**Residual Stress**
0.18	10.98	2.923
0.36	21.96	13.903
0.70	42.7	34.643

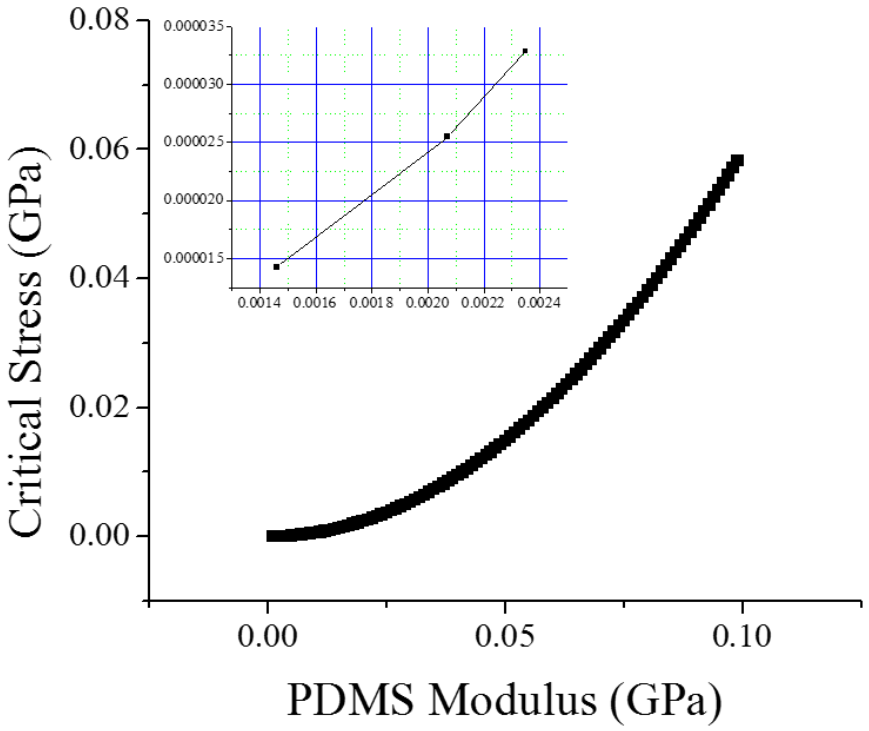

Figure 5.8: Dependence of (a) profile wavelength on critical stress (b) substrate modulus on critical stress.

5.5 Computational Model Results

5.5.1 Buckling Profile as a Function of Pre-Strain and Substrate Elastic Modulus

The von Mises stress of the Au/PDMS structure showed a dependence of substrate elastic modulus on stress distribution and profile amplitude. The increase in the elastic modulus of the substrate increases the concentration of stress in the buckled structure. Also, the buckling profile becomes well defined as the elastic modulus of PDMS increased. The wavelength was measured as function of pre-strain in table 5.4. Comparing computational results to experimental results showed insignificant difference.

Table 5.4: Results wavelength measurement as a function of pre-strain

Pre-strain	**Wavelength (μm)**		**Amplitude (μm)**
	Experimental	Computational	Computational
0.18	9.70	9.54	0.35
0.36	6.60	7.30	0.30
0.70	3.00	4.30	0.28

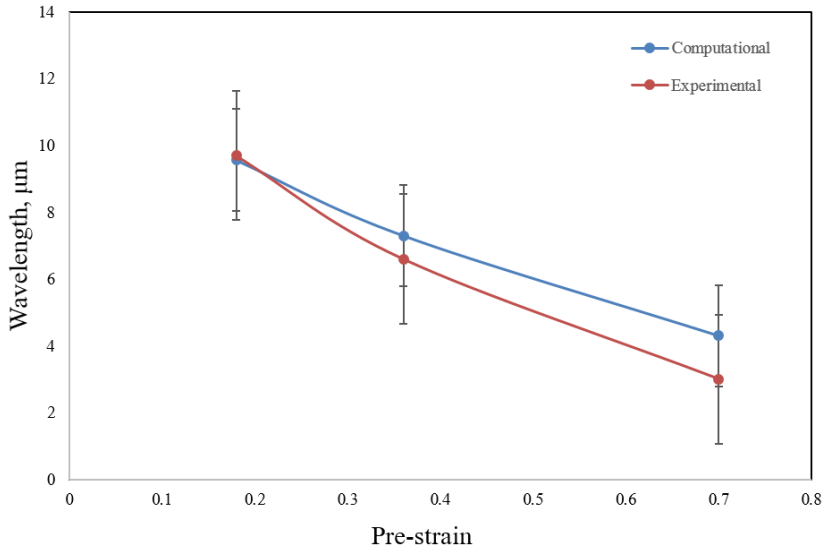

Figure 5.9: The wavelength of the profile versus pre-strain value of the PDMS substrate.

5.6 Effect of Surface Modification on Cell Adhesion

The effect of surface modification on cell adhesion was measured as a function of energy release rate. A graph of energy release against substrate modulus was plotted in Fig 5.10. For PDMS substrates with different moduli, the energy release rate decreased with increasing modulus. When the silica layer was introduced onto different substrate, the

same trend was observed. Silica layer on PDMS with stiffness of 1.46 MPa had a higher energy release rate than PDMS with stiffness of 2.35 MPa. Also it was observed that the stresses were virtually on the silica layer (Figure 5.11). The energy release rate is the energy associated with a new fracture surface created. A higher energy release rate implies a larger crack opening. Hence decreasing energy release rate implies that as the stiffness of PDMS substrate increased, the cells did not detach. This is an indication that as PDMS stiffness increased, cell adhesion was enhanced. Also the silica layer on the PDMS decreased the energy release rate even the more. This is because higher stiffness of the silica was sensed by pulling and pushing it, and transduce the force into biochemical signals in response (mechanotransduction process). Higher substrate stiffness tends to increase cell adhesion.

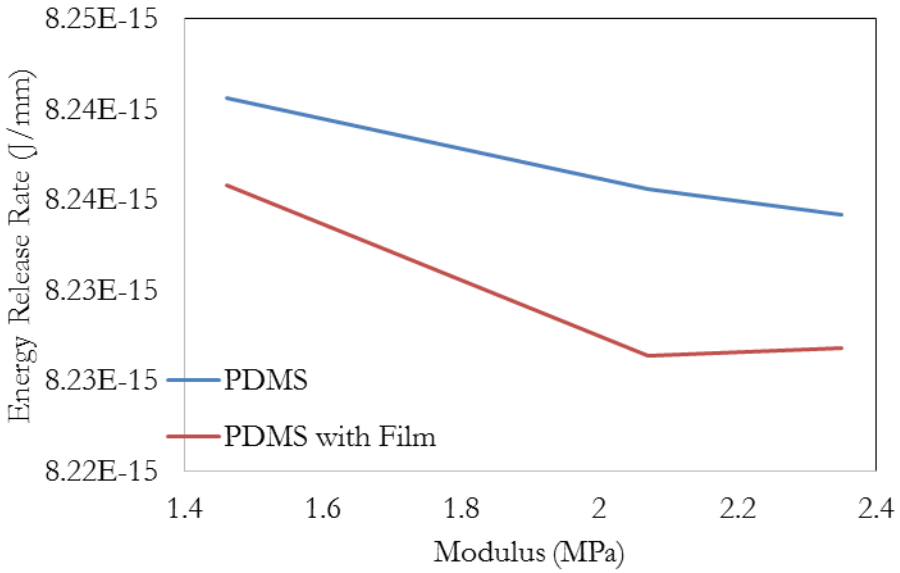

Figure 5.10: Cell detachment as a function of Energy Release Rate

(a) (b)

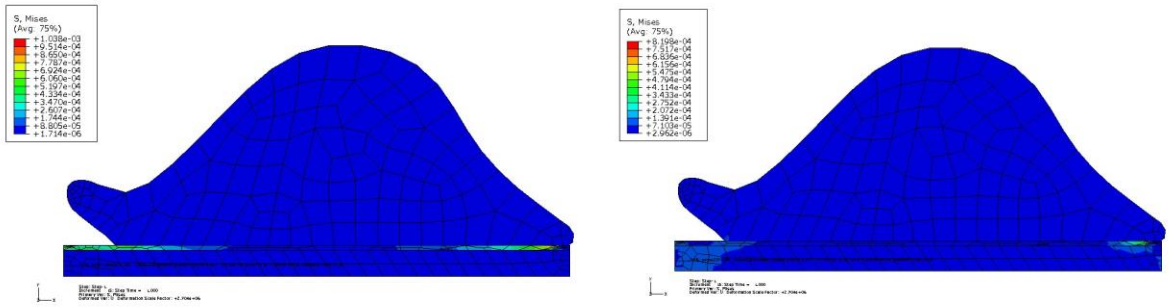

Figure 5.11: Cell detachment from (a) PDMS with silica layer, (b) PDMS with stresses concentrated on PDMS with silica layer

5.7 Reference for chapter five

[1] W. D. J. Callister and D. G. Rethwisch, “Materials Science”, Seventh. New York: John Wiley & Sons, Inc, pp. 1–975, 2007.

[2] D. J. Campbell, K. J. Beckman, C. E. Calderon, P. W. Doolan, R. H. Moore, A. B. Ellis, G. C. Lisensky, “Replication and Compression of Bulk Surface Structures with Polydimethylsiloxane Elastomer.” :Uses of Polydimethylsiloxane (PDMS) Elastomer, J. Chem. Educ. Vol. 76, 537, 1999.

[3] Z. Wang, A. A. Volinsky, N. D. Gallant, “Crosslinking Effect on Polydimethylsiloxane Elastic Modulus Measured by Custom-Built Compression Instrument,” J. Appl. Polym. Sci., vol. 131, 41050, 2014

[4] K. Efimenko, W. E. Wallace, and J. Genzer, “Surface Modification of Sylgard-184 Poly (dimethyl siloxane) Networks by Ultraviolet and Ultraviolet / Ozone Treatment,” vol. 315, pp. 306–315, 2002.

[5] C. L. Beyler, and M. M. Hirschler, “Thermal decomposition of polymers,” in SFPE handbook of fire protection engineering, vol. 2, 2002.

[6] M. A. Brook, “Silicon in Organic, Organometallic, and Polymer Chemistry,” J. Wiley, New York, p. xxiv, 680, 2000.

[7] J. Yull, D. Ahn, Y. Young, C. Mo, S. Takayama, S. Hyuck, and S. Lee, “Surface chemistry modification of PDMS elastomers with boiling water improves cellular adhesion,” Elseveier Sensors Actuators B Chem., vol. 173, pp. 765–771, 2012.

6.0 CHAPTER SIX

6.1 Implications of the Results

The Physiochemical properties of modified PDMS substrates draws much attention its performance as a support for cell adhesion and growth. The various surface modifications that have been used in this work have resulted in PDMS substrates being patterned with chemical or topographic features. It has been established that patterning of surface with chemical or topographical features enhances cell adhesion, hence the results of PDMS surface modification implies improved cell adhesion and subsequent integration as a biomedical implant device.

PDMS substrates treated via boiling water and UVO showed significant chemical feature by generating OH group which reliefs PDMS of its hydrophobicity. Prior work [1] have showed that, making PDMS hydrophilic led to significant increase in the number of cell growth. This implies that the hydrophilic PDMS surface created by boiling and UVO treatment will enhance cell adhesion. Hydrophilic surface allows cell attachment proteins (vitronectins and fibronectin) to adhere and spread providing better surface for cell adhesion. Also, Kirill et al., [2] reported a uniform silica-like layer of higher stiffness formed on UVO-PDMS, with a thickness of about 10-30 nm. The implication of this to this current work is an enhanced cell/surface interaction since cells are able to sense substrate stiffness.

Coating of Au on PDMS have resulted in buckling profile with micro- groove, and wavelength and amplitude on a micro scale. This has been validated in the current work, where effects of increasing pre-strain led to a decrease in wavelength of buckling profile from 9 to 3μm. It has been reported that to precisely control the cell location and growth,

it is desirable to use a micro-pattern with size similar to the cell [3]. Analytical and computational methods can thus be used to determine stressed required to modify the surface of PDMS. Also, these can be used to predict the limiting pre-strain that will yield desirable patterns for enhanced cell adhesion.

These results imply that encapsulating targeted delivery drug in modified PDMS is a step in the right direction. Since PDMS is already biocompatible, and by these modifications, the issues of poor cell adhesion as a result of its smoothness and hydrophobicity is addressed.

6.2 Conclusion

This work presents the results of a combined experimental and computational study of the PDMS surface modification. The chemical modifications were measured with FTIR which showed results of OH group on PDMS surface, with formation of silica layer. Increased PDMS stiffness is improves cell adhesion to an extent.

By chemically and physically modifying PDMS, different length scale modification occurs, leading to cell-surface interaction on a multi-scale. Higher detachment forces required to detach cells from modified surface indicates improved cell-surface interaction.

The enhanced cell adhesion will results a better integration when PDMS is used as a microfluidic device for localized drug delivery.

6.3 Future Work

It is recommended that, for chemistry modification such as generation of hydroxyl group on PDMS surface, more sylgard base and little amount of crosslinking agent be used.

This will lead to uncross-linked SiH, which can easily form OH group and make PDMS hydrophilic.

Further studies is required to determine optimal time for UVO treatment to eliminate. Also optimal hydrophilicity and hydrophobicity required for cell adhesion should be established to guide modification methods used for PDMS.

6.4 Reference for Chapter Six

[1] C. Jensen, L. Gurevich, A. Patriciu, J. Strujik, V. Zachar, and C. P. Pennisi, "Stable Hydrophillic PDMS surfaces produced by Plasma treatment for Enhanced Cell Adhesion," 15th NBC on Biomedical Engineering and Medical Physics, IFMBE Proceedings 34, pp. 105-1-8, 2011.

[2] K. Efimenko, J. A. Crowe, E. Manias, D. W. Schwark, D. A. Fischer, J. Genzer, " Rapid formation of soft hydrophilic silicone elastomer surfaces," Journal of Polymer Science, vol. 46, pp. 9329-9341, 2005.

[3] J. Hu, C. Hardy, Chi-Mon Chen, S. Yang, A. S. Voloshin, and Y. Liu, "Enhanced Cell Adhesion and Alignment on Micro-Wavy Patterned Surfaces," Plos One, one 9.8: e104502, 2014.